

國立臺灣大學理學院地質科學研究所

碩士論文

Graduate Institute of Geosciences

College of Science

National Taiwan University

Master Thesis



Geological and Geochemical Analyses for Emerald Exploration in  
the Muzo Formation along the Western Emerald belt, Colombia

凡凱培

Gabriel Felipe Nino Vasquez

指導教授：宋聖榮 博士

Advisor: Sheng-Rong Song, Ph.D.

中華民國 106 年 7 月

July, 2017

國立臺灣大學碩士學位論文  
口試委員會審定書

Geological and Geochemical Analyses for Emerald  
Exploration in the Muzo Formation along the Western  
Emerald belt, Colombia

本論文係凡凱培君（學號 R04224117）在國立臺灣大學地質科學研究所完成之碩士學位論文，於民國 106 年 7 月 10 日承下列考試委員審查通過及口試及格，特此證明

指導教授：

吳鳳華

口試委員：

王珮玲

陳惠芬

林卉婷



## ***ACKNOWLEDGMENTS***

*I am grateful to the National Taiwan University for the opportunity to study this Master's degree in geosciences. Secondly, I want to thank my tutor Sheng-Rong Song for his unconditional support in both academic and logistics issues. I offer great recognition to Blake Becher, without whose help it would not have been possible to visit the different emerald mines. His economic and logistical support were fundamental for the development of this research. To John Coates for his disinterested and timely collaboration in the revision and correction of my manuscript Finally, I would like to sincerely thank 廖陳侃, since he was an unconditional friend and colleague during my Master's studies.*



## ABSTRACT

The Colombian emeralds are distributed in two parallel belts where the host rocks are mainly Cretaceous black shales and limestones. A better understanding of the mineralizing processes which form the emerald deposits in Colombia will improve the exploration activities within both belts.

This study focuses on the Western Emerald Belt (WEB) where seven mines were visited. The WEB is located in the central part of Colombia, on the western flank of the Eastern Cordillera. The most important emerald mines are located in Muzo, Maripi, Yacopi, Otanche and Coscuez municipalities.

Thirty-six samples were collected for analyses of carbon and oxygen isotopes with the purposes of: first, to know the main source of the fluid(s) which interacted with the shales in order to form the emeralds and associated minerals (pyrite, calcite, chalcopryite, quartz, albite, etc.), and second, to identify if the analyses of stable isotopes combined with field and laboratory information are determinant and useful for the exploration of emeralds in the WEB. Geological information such as structural data, identification of debris flows, hydrothermal and hydraulic breccia as well as mineral assemblage were collected during the field trip. For microscopic analyses, 17 samples were characterized by petrographic observations, such as microstructures, mineral habits, paragenesis and deformation parameters. The identification of different carbonates and supergene minerals was conducted with a RAMAN spectrometer and Scanning Electron Microscope (SEM).

The main conclusions of this research suggest that: 1. the mineralizing fluids came from a metamorphic / sedimentary origin. 2. A range for  $\delta^{18}\text{O}$  (SMOW) between 18 to 21.8 ‰ and -4 to -10.3 ‰ for  $\delta^{13}\text{C}$  (PDB) represents the isotopic signatures of the hydrothermal fluids which produced the emerald mineralization for the visited mines. 3. Calcites from the Muzo Formation in the WEB would have the possibility of being associated with emeralds, if apart from being in the previously mentioned ranges of isotopic values; the carbonate is in paragenesis with sulphides, albite and/or quartz originating from either hydrothermal or hydraulic breccia associated with thrust planes, folds and overthrust faults. For exploration purposes, it is important to define debris flows to avoid mining development in such areas.

**KEYWORDS:** WEB, hydrothermal-sedimentary deposits, emerald, Muzo Formation, isotopic fractionation, subduction



## Table of Contents

<b><u>1. INTRODUCTION</u></b>	<b>1</b>
<b><u>1. LOCATION</u></b>	<b>2</b>
<b><u>2. METHODOLOGY</u></b>	<b>6</b>
2.1 BIBLIOGRAPHICAL REVIEW	6
2.2 FIELD WORK AND SAMPLE COLLECTION	6
2.3 LABORATORY WORK	7
<b><u>3. GEOLOGY</u></b>	<b>8</b>
3.1 LITHOSTRATIGRAPHY	10
I. FURATENA FORMATION	10
II. MUZO FORMATION	11
III. CAPOTES FORMATION	12
3.2 STRUCTURAL GEOLOGY	12
I. RIO MINERO FAULT	13
II. ZULIA- ALBANIA FAULT	13
III. PAUNA ANTICLINE	13
IV. EL ALMENDRO SYNCLINE	13
<b><u>4. MINES DESCRIPTION</u></b>	<b>14</b>
4.1 GROUP 1	15
4.1.1 MONTEBLANCO MINE	15
4.2 GROUP 2	18
4.2.1 LA PITA	18
4.2.2 CUNAS	24
4.2.3 ESPAÑOLES	27
4.3 GROUP 3	30
4.3.1 COSCUEZ	30
4.4 GROUP 4	32
4.4.1 MASATO AND PUERTO SIAD	32
<b><u>5. MINERALOGY AND GEOCHEMISTRY</u></b>	<b>35</b>
<b><u>7. DISCUSSION AND CONCLUSIONS</u></b>	<b>67</b>
<b><u>8. REFERENCES</u></b>	<b>73</b>

## 1. INTRODUCTION

Colombia is located in the northwest of South America where three tectonic plates actively interact (Nazca, South American and Caribbean plates). The Andes Cordillera is the main product of this interaction. In consequence, Colombia hosts a large quantity of mineral resources; and emerald deposits are one of the most important and iconic.

Emerald is a variety of beryl ( $\text{Be}_3\text{Al}_2(\text{SiO}_3)_6$ ) with traces of chromium (Cr) and vanadium (V), which provide the characteristic green colour to the mineral. The emeralds in Colombia are located in two parallel belts of the Eastern Andes Cordillera, separated by approximately 130 km: namely the Western belt (WEB) and the Eastern belt (EEB). The geological, mineralogical and tectonic features from these belts are quite similar, but the age for the WEB is 38 Ma (Cheilletz et al., 1994) and 65 Ma for the EEB (Cheilletz et al., 1995).

Previous researchers analyzed oxygen, carbon, and sulphur isotopes taken from quartz and carbonate in mine deposits from both belts. They concluded that emeralds in Colombia originate from hydrothermal sedimentary processes without any magmatic influence (Cheilletz et al. 1995) which make these deposits unique around the world. They also suggested that the source of chromium (Cr), vanadium (V) and beryllium (Be) is from the host rock (Cretaceous black shales).

The study of stable isotopes has been useful to determine the conditions of the mineralizing fluid, however, is it useful to analyse these isotopes for the exploration of emeralds in the WEB?

The present thesis focuses on identifying if the analyses of stable isotopes (carbon and oxygen), combined with geological observations gathered from the field trips and laboratories, are determinant and useful for the exploration of emeralds in the WEB. For this purpose, isotopic analysis was performed on 36 samples of calcite from 7 different mines, covering both productive and none productive areas from the Muzo Formation. In addition, it is necessary to compare, identify and characterize the fluid-rock interactions in different sectors of the WEB in order to determine whether the fluid, which is highly oxidizing and saline (Giulliani 1994) (Ottaway 1995)) is similar throughout all the mines or if the composition and therefore its efficiency to leach trace element constituents from the shale differs across the sample suite.

This research is important and significant, because emeralds are very important for Colombia, in relation to their high economic value as well as being an important cultural heritage. A better understanding of emerald genesis would facilitate the searches for more possible deposits.

## **1. LOCATION**

All the samples were collected along the Western Emerald Belt (WEB) which is located in central Colombia, in the western parts of Boyacá, Cundinamarca and Santander departments. The most important population centre are Muzo, Maripi, Yacopi, Otanche and Coscuez. (Fig. 1).

Geographically, the WEB is located on the western flank of the Eastern Cordillera. Morphologically the whole area is mountainous and is characterized by moderate to strong relief, with medium density

sub-parallel and sub-dendritic drainage and development of juvenile valleys. In some sectors, the topography is softened by the presence of Quaternary deposits, mainly of high energy fluvial origin. The rivers that drain the area belong to the watershed of the Magdalena River. The most important are the Canutillo, Ibacapí, Piedras, Minero, Chinche, Tambrias, Murca and Patá rivers. The maximum height is 2,450 m. S. N. M. while the minimum is of 250 m. S. N. M (Reyes, 2006).

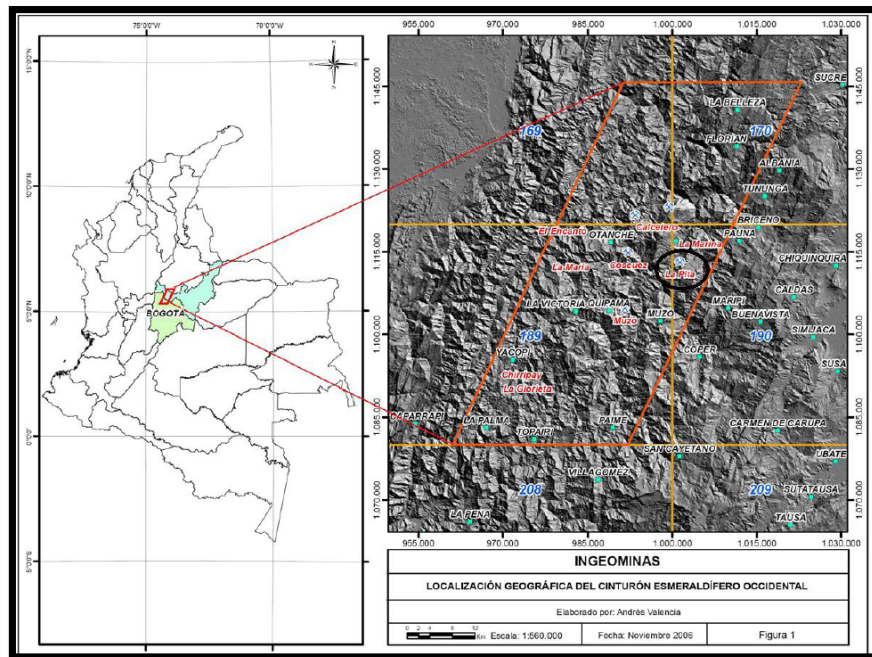


Figure 1 The location of Western Emerald Belt (WEB). Modified from Reyes 2006.

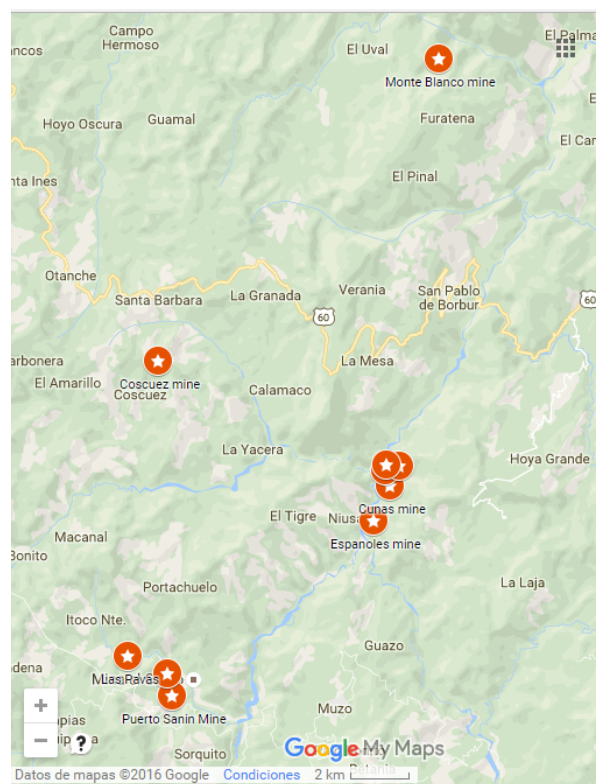


Figure 2 Distributions of Visited mines.

Sample	Mine	Location	
		x (Latitud)	y (Longitud)
2 7 8	La Pita (Divino Niño)	5.603	-74.084
4 9 10 11 14 15 16 17 18 19 23 26 27	La Pita (Mecanizado 2) La Pita La Pita La Pita La Pita La Pita (Trapiche #1) La Pita (Trapiche #1) La Pita (Trapiche #2) La Pita (Trapiche #2) La Pita (Trapiche #2) La Pita (Nivel 3) La Pita (Trapiche 2) La Pita	5.603	-74.088
28 30 31	Coscuez	5.634	-74.155
32 33	Monteblanco	5.722	-74.073
35 36 37	Cunas	5.597	-74.087
38 39 40 41 43 45 46	Espanoles	5.586	-74.092
49 51	Puerto Siad	5.535	-74.151
54 55 56	Masato	5.542	-74.153 - -

Table 1 Cartographic coordinates for the sampled mines.

The samples collected for this study come from 7 different mines along the WEB (Fig. 2). The cartographic coordinates for each mine are summarized in Table 1. (There are 8 cartographic coordinates since two exploration tunnels were sampled at the La Pita mine).

## **2. METHODOLOGY**

### **2.1 BIBLIOGRAPHICAL REVIEW**

The work done by different authors on the formation of emeralds not only in Colombia but also around the world was reviewed. The bibliography includes works of geological cartography, petrography and especially analyses of stable isotopes in order to analyze and compare the results obtained through this research with others. Basic texts and updated articles of Cretaceous basin formation in Colombia, geochemistry, ore deposits from hydrothermally altered sedimentary rocks, and petrogenetic models for the formation of beryl were also studied.

### **2.2 FIELD WORK AND SAMPLE COLLECTION**

The field work was carried out in the summer of 2016 and with the accompaniment of the professor-advisor Sheng-Rong Song, the geologist Rory Kutluoglu and the classmates 廖陳侃 and 林坤誼. Eight emerald mines along the WEB were visited and sampled during a period of three weeks. The main purpose was to understand the geological processes in the area, by sampling both altered and unhydrothermally altered host rocks, as well as mineralized and sterile zones. Structural data for the bedding and veins were taken where it was possible.

## 2.3 LABORATORY WORK

For a proper geochemical analysis, 17 representative samples of the mines were selected for a petrographic analysis under the optical microscope and scanning electron microscopy (SEM). The 17 samples were prepared, analyzed and classified in the laboratories of the Department of geosciences, National Taiwan University.

For the analyses of stable isotopes, calcites from veins, rocks, and breccia were selected. Since there are other carbonates such as dolomite, ankerite, codazite, etc. present with the emerald mineralization, it was necessary to use the Scanning Electron Microscopy (SEM) for the calcite separation. The SEM used for the analyses is a Quanta 200 Feg with an Energy Dispersive X-ray Spectrometer (EDS) from the Department of Geosciences, National Taiwan University.

The carbon and oxygen isotopic compositions of calcites were analyzed by a Thermo-Scientific MAT 253 Isotope Ratio Mass Spectrometer (IRMS), equipped with an automatic Carbonate Device (Kiel) at the Institute of Oceanography, National Taiwan University.

Supergenic sulfates found on the walls of the mines were analyzed and classified in a FHR 1000 RAMAN spectrometer with a  $> 300$  nm/second scanning speed at the Department of Geosciences of the National Taiwan University. This technique was also implemented for the classification of the different carbonates.



### 3. GEOLOGY

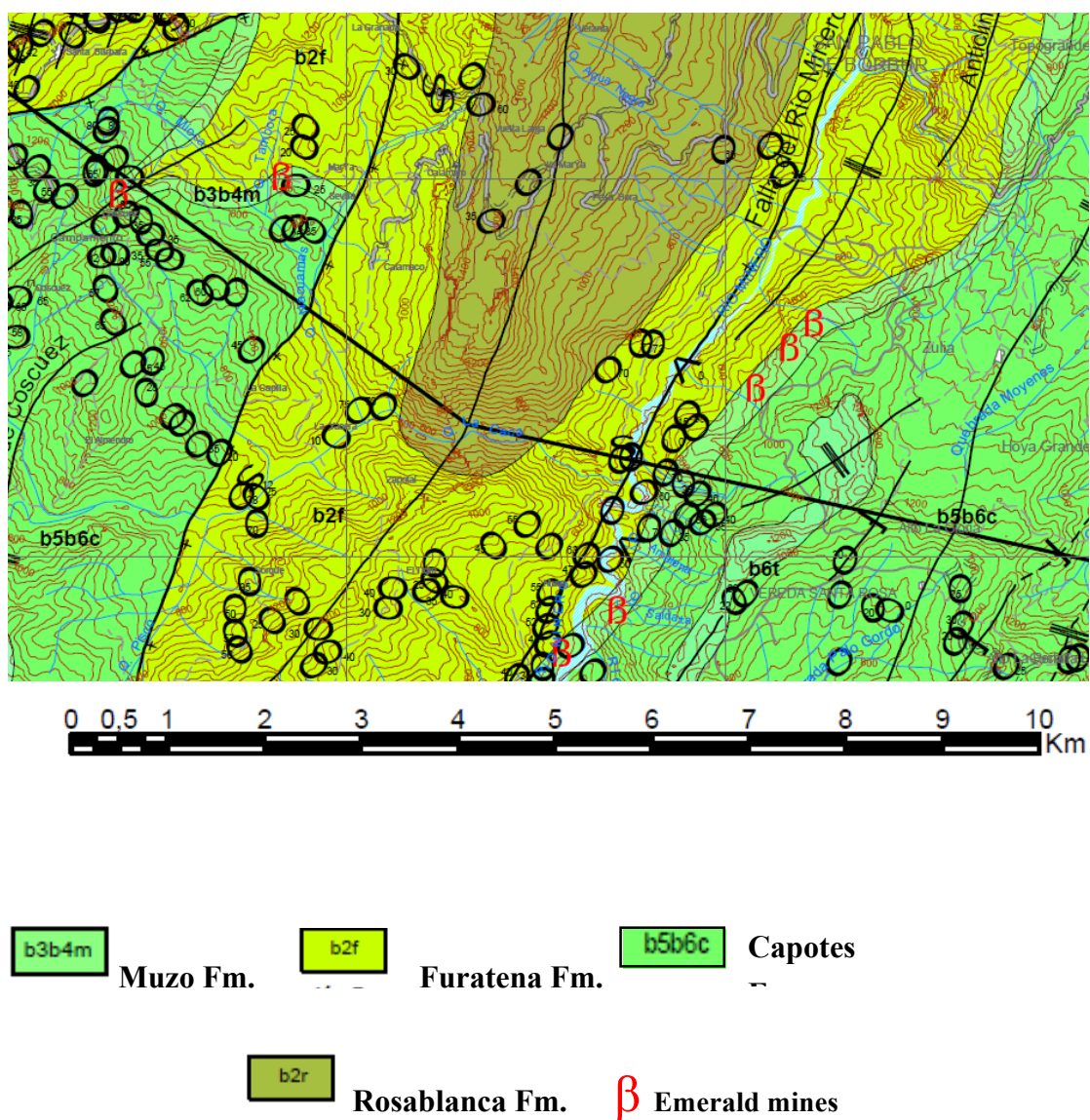
The western emerald belt, located in the central part of the Eastern cordillera, contains a fairly complete lithological record of Cretaceous transgressive sedimentation. Within a facies distribution scheme, the sedimentary subsidence must have played an important role along the distending faults that are currently manifested in reverse or transcurrent regional faults, due to tectonic inversion. These manifestations are in both NE and NW orientations.

The geometry of structures in general does not respond to a pure faulting system, but is a combination of inverse and transcurrent faults. Often, the folds end diagonally against the faults, indicating transcurrent movement. There are overthrust blocks, in which the fault throws have been determined by biostratigraphic analysis, however usually the thrust faults do not have a morphological expression (Reyes, 2006).

In the study area, Lower Cretaceous sedimentary rocks outcrop (Fig. 3). The muddy composition of the units influences the tectonic deformation of the rocks through their ductile behaviour, and generates intense folds and faults which are not easy to recognize. The folding is common at both regional and local scales. The anticlines that separate them are not well defined and they present very tight and generally asymmetric closures (Reyes, 2006).

Due to the high dip angles of the sedimentary layers, and the steep relief due to high rates of erosion, denudation of the terrain and landslides causing huge debris flow deposits commonly obscure bedrock and complicate exploration and exploitation of beryl. Many mines are established in these debris flow

deposits which are not suitable for a large scale exploration of the emeralds since there is no continuity or stratigraphy of the mineralizing veins. In this study, it is proposed to study landslides along the WEB to define areas covered by debris flow, which may overlie hard rock sources. Thus, mineralised debris flows need to be interpreted and the source bedrock of the mineralised structures traced.



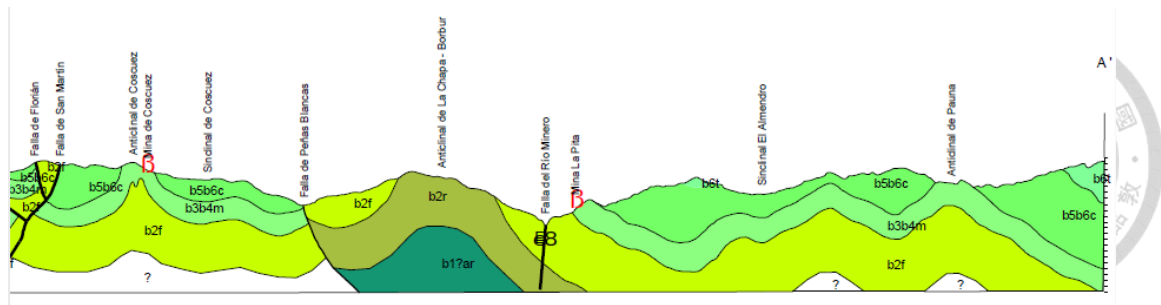


Figure 3 Map and geological profile of the study area. Modified from Reyes 2006.

### 3.1 LITHOSTRATIGRAPHY

Although the emeralds in the WEB in Colombia occur in both the Rosablanca and Muzo Formations, all the emerald mines visited in the summer of 2016 are within the Muzo Formation. All the geological formations involved in the area are dominated by sedimentary rocks, with lateral changes in the lithology. Below there is a description of each formation from the oldest to the youngest one.

#### I. Furatena Formation

The Valanginian Furatena Formation (Etayo 2005 and Reyes 2006) is a sedimentary unit, composed mainly of fine-grained rocks, underlain by the Rosablanca Formation and overlain by the Muzo Formation. According to INGEOMINAS-GEOERESOURCES EXPLORATION LTDA (2005) and INGEOMINAS - GEOSERCH LTDA (2005) (Reyes, 2006) the Furatena Formation is defined as layered claystones and siltstones with some sectors where siliceous material predominates. The lowest segment 1 is formed by thick claystones followed by accumulation of organic matter. Segment 2: intercalations of claystones and mudstones with common gypsum, disseminated pyrite and iron oxides. Segment 3: at the base is composed of mudstone, sometimes siliceous, followed by siltstones in

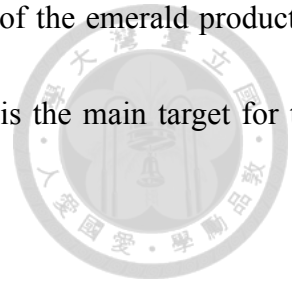
medium and thick layers, towards the middle and upper layers. Thick limestone, calcareous, micrites and lenses of coal. Segment 4: is a muddy sequence where some intercalations of sandstones and siltstones are observed. Segment 5: tabular layers of claystones and mudstones. Segment 6: composed of limestone and mudstones. (Reyes, 2006).

## **II. Muzo Formation**

Muzo is a Hauterivian-Barremian Formation which is formed by calcareous and non-calcareous sequences. Underneath the Muzo Formation is the Furatena Formation and overlying is the Capotes Formation (Etayo, 2005 and Reyes 2006). There are several differentiable segments within this Formation:

- Segment 1: This is a range of limestones (mainly mudstone) with intercalations of non-calcareous mudstone.
- Segment 2: An interval consisting of intercalations of siliceous mudstone and siltstone (shales).
- Segment 3: quartz sandstones, shales and siliceous mudstones.
- Segment 4: mudstone and calcareous and non-calcareous shales with micritic limestones and immature quartz sandstones with calcareous cement.
- Segment 5: Formed by gray-colored mudstones with sandy silstones and micritic limestones.
- Segment 6: Consisting of sandstones and muddy sandstones, with calcareous cement and siliceous mudstones; in addition, pyrite, silty, siliceous and calcareous nodules are present as

well as calcite veins (Reyes, 2006). The Muzo Formation is one of the emerald productive Formations along the WEB, and the mineralization hosted there is the main target for this research (Fig. 4).



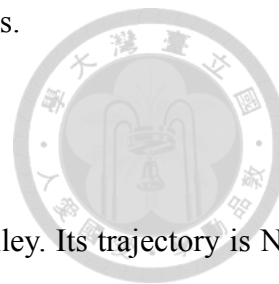
### **III. Capotes Formation**

Capotes is an Aptian-Albian Formation (Etayo 1979, Reyes 2006), which is composed of a succession of fine grained rocks, comprising claystones, shales and sometimes marls. In the study area the Capotes Formation is formed by layers of mudstone and claystone with calcareous concretions, some with ammonites. Concretions filled by pyrite of considerable diameter 30-80 are commonly found cm. (Reyes, 2006).

### **3.2 STRUCTURAL GEOLOGY**

The Western Emerald Belt is a structurally complex region due, in part, to the ductility of the underlying sediments. This makes it a highly faulted and folded area. However, in the field, it is not easy to identify the faults, since the rock is so fractured and altered. It does not clearly show breaks between the blocks or the characteristics of a fault zone as fault gouges, mylonites or cataclastic rocks. Sometimes what appears to be a contact between two blocks is a contact between in situ rock and debris flows. This can also create confusion with zones of hydraulic fracturing suffered by the rocks due to the pressure of the mineralizing fluid. In some sectors the shale is very altered by the hydrothermal fluid, being reduced to kaolin which can obscure the structural characteristics of the rocks.

Our sampling sites are under the influence of two major faults and two folds.



### **I. Rio Minero Fault**

Its name derives from the Minero River and is sub-parallel to the river valley. Its trajectory is N20°-35°E and is rectilinear with some small variations in its course. Movement is predominantly dextral; and is revealed by the juxtaposition of different stratigraphic assemblages across the fault (Reyes, Germán et al., 2006).

### **II. Zulia- Albania Fault**

It is a sinistral NW-SE regional fault, with an important inverse jump (northwest vergence) (Reyes, 2006).

### **III. Pauna Anticline**

It is one of the most extensive folds in the area and is oriented NNE-SSW. To the northeast it is truncated by the Zulia-Albania fault. It is a symmetrical structure and in its core there are Valanginian and Barremian rocks of the Furatena and Muzo Formations outcrop (Reyes, 2006).

### **IV. El Almendro Syncline**

This is a regional structure which terminates to the west against the Ibacapí fault. Located in its core is the Zulia Police Inspection station. The rocks are lithologically resistant to erosion and can be seen in the Alto Camacho and Panache hills. The hinge surface is oriented N30°E. It is an open and sub-vertical syncline (the hinge surface dips 85° to the southeast) (Reyes, 2006).

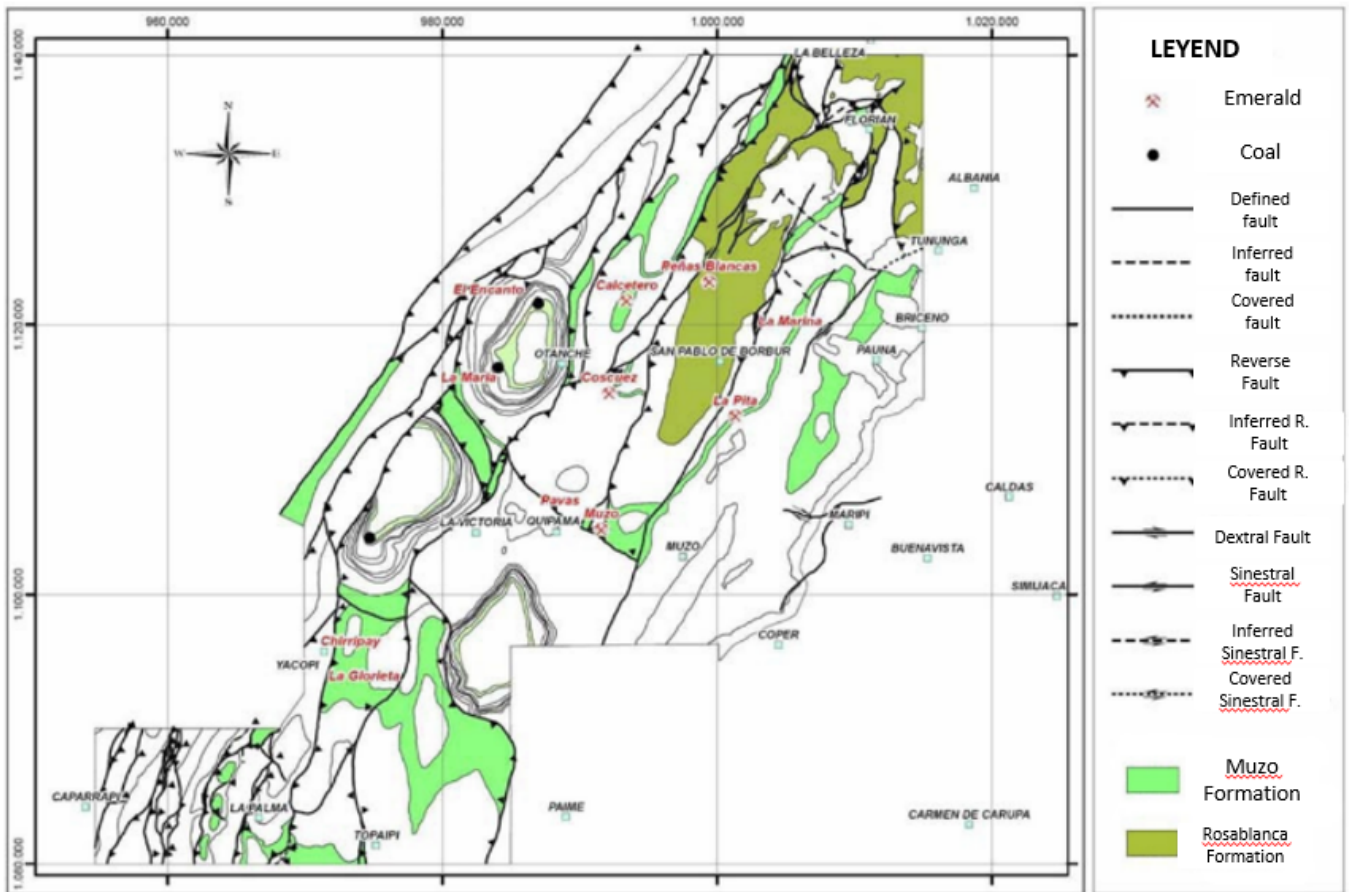
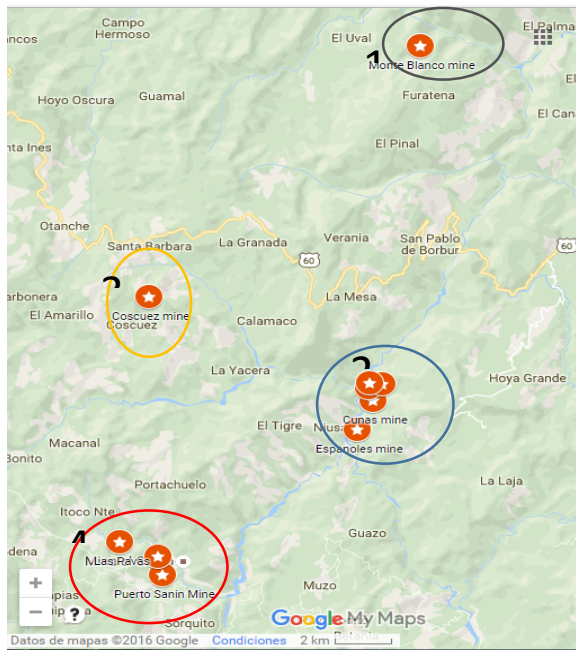


Figure 4 Structural map and productive formations along the Western Emerald Belt. Modified from Reyes 2006.

#### 4. MINES DESCRIPTION

The geological description of all the visited mines and the petrographic analyses under the optical microscope are included in this section. There are some previous studies from some of the mines which are also considered in the current research. Note that all of the visited mines are hosted in Muzo Formation.

For a better understanding of the mines' geological features, the area was divided into four different groups as shown in the map below (Fig. 5).



Group	Mines Name
1	Monte Blanco
2	La Pita
	Cunas
	Espanoles
3	Coscuez
4	Las Pavas
	Puerto Sanin
	Masatos

*Figure 5 Mines groups location.*

## 4.1 Group 1

### 4.1.1 Monteblanco Mine

This is the most northerly visited mine, located in El Uval municipality. Currently the mine is under exploration. The mine is being explored along a single tunnel, using an empirical approach and without any professional or scientific support. The tunnel entrance is located at the base of a mountain with a fairly steep slope, next to a small juvenile river that forms a pronounced "v" shaped valley. It is evident that the flow of landslides, (debris flows) from the upper slopes are the predominant surficial deposits.

The tunnel has a depth of approximately 200 meters but it has not yet reached bedrock. Only debris flow has been cut; at times containing large blocks of rock that reach up to 10 meters wide. There is no continuity in the veins, and there is no defined strike of the layers for the shales.



Investigating geochemistry and petrography in the area, two calcite samples were collected, one in rock (Sample 32) and one in vein (Sample 33). The samples are not assumed to be associated with the mine since these blocks could have been transported from the top of the mountain to the current place as the rock is not in-situ.

No gem emeralds have yet been found in the mine. According to the miners only "murralla" which is the mining term that defines the emerald of low quality has been identified.

In this study, in order to define productive and non-productive zones, the mine is not considered to be an economically viable area. In fact, it is believed that the risk of exploiting the sector is high as it is prone to landslides (Fig.6).



*Figure 6 (Left) flow of landslides in the Monteblanco area, the mine entrance is at the bottom of the mountain. (Right) debris flow deposits inside the mine.*

#### 4.1.1.1 Microscopic observation

**1.1.1.1.1** Sample 32: The sample was collected from the shale in contact with the carbonate. Overall, the shale shows a carbonaceous alteration due to the interaction between the rock and the hydrothermal fluid. Microcrystals of quartz, carbonate and plagioclase contained within the rock were identified. Sometimes bigger quartz crystals with wavy extinction are found in the shale, signaling higher pressure (Fig. 7). The carbonate shows a wavy extinction with very high order colours under crossed-nicol observations. The relief changes with rotation and is very high, showing the perfect rhombohedral cleavage. The lamellar twins are quite evident and on PPL the mineral is colourless. In Figure 8, it is possible to see a “granoblastic” texture in the calcite. Under the microscope, it is easier to see different growth stages within the calcite than with the naked eye, since successive carbonate veins, usually cross cut each other.

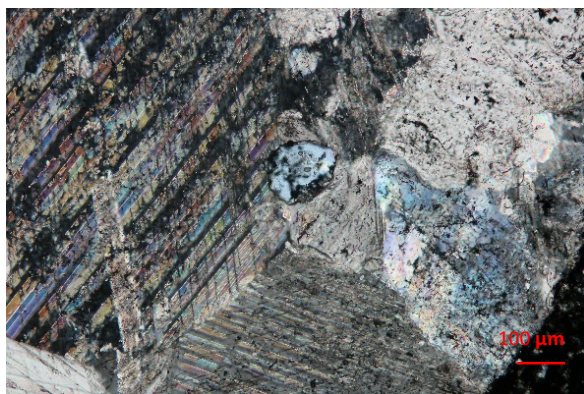


*Figure 7 Different stages for the carbonate. Xpl.*

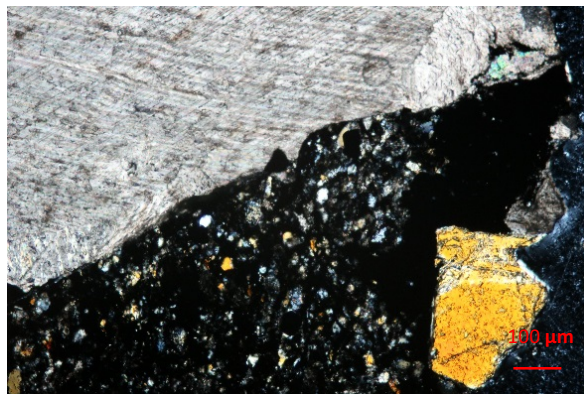


*Figure 8 Carbonate in contact with the black shale. Xpl.*

## 4.2 Group 2

Espanoles, Cunas and La Pita are categorized into group 2. This sector lies along the road from Maripi to Muzo. The mines are located on the slopes of the Muzo River and are crossed by the Muzo fault that in this sector brings together blocks of the same geological formation (Muzo Formation).

This sector is very notable for both exploration activities and exploitation of emeralds and currently produces one of the best qualities of emerald in the world. Of the mines visited, these three are the largest and most productive.

### 4.2.1 LA PITA

The mine has in its outermost part, joints with two predominant families in directions E-W / 45-50°S and N10-20°W / 85-90°SW (Fig. 9). The joints are the products of both, the mechanical weathering due to the high temperatures that are reached during the day, and due the compressional movements typical in the Andes Cordillera Andean movements. In the underground areas, the demarcation is not so pronounced due to the ductility of the rock, which increases the leaks of flow of large quantities of groundwater, which gives rise to one of the most important problems facing the exploitation (Puerto, 2012). Also within the galleries are small local folds (Fig. 10).



*Figure 9 Joints with two predominant families in directions E-W / 45-50°S and N10-20°W / 85-90°SW.*



*Figure 10 Recumbent folds showing that the area has been subjected to constant efforts that caused the deformation of the rock.*

The La Pita mine Exploration-exploitation follows the direction of the Muzo fault towards the north (Fig. 11). Currently, La Pita is being mined only on the footwall block. Mineralization within the gallery are presented in the form of veins with the presence of different mineral associations such as carbonates, albite, metallic minerals (such as pyrite and chalcopyrite), fluorite some oxides, sulfides and quartz (Fig. 12).



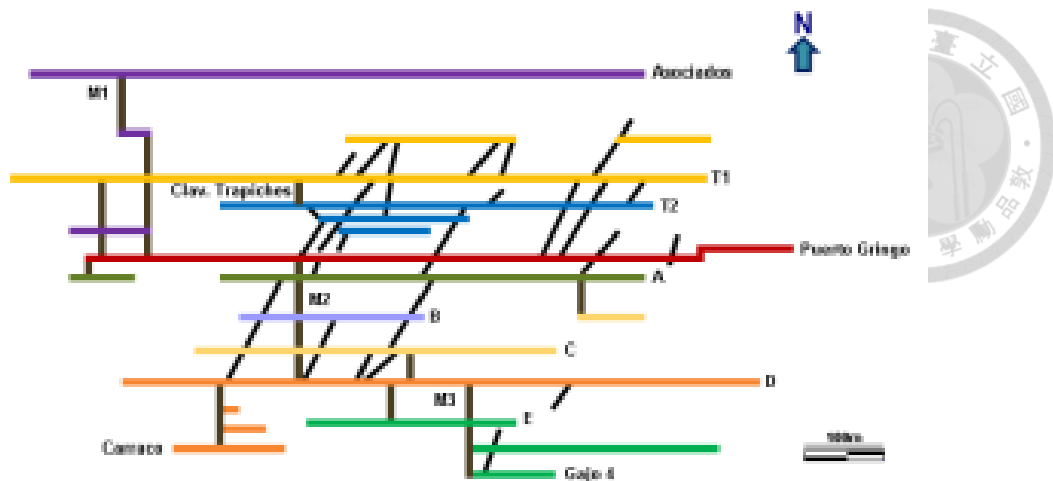


*Figure 11 Profile showing the different fronts of exploitation of La Pita, the miners guide the mine in the direction of the fault of the Minero River. The mine has a depth of approximately 300 meters. The profile is courtesy of Promina de Zulia S.A.*



*Figure 12 Emerald from La Pita associated with Carbonate and pyrite.*

The producing areas are veins that vary in thickness from a few centimetres up to 2 meters wide (Fig. 13). The veins are found erratically throughout the mine. However, it should be noted that there are two preferential orientations for the veins; one with a strike to the SE and another with a strike to the NE. The mine is being explored and exploited following the contact between the unaltered shale and

the hydrothermally altered shale which is identified as a hydrothermal breccia. The clasts within the breccia are euhedral to anhedral carbonate at different stages, the order is chaotic, clast-supported to matrix-support, fine to very coarse unsorted sharp clast contacts. The last stage is altered to a kaolinite overprint. (Fig. 14).



*Figure 13 Veins with sizes ranging from a few centimeters to 2 meters. The orientation of the veins is not random. However, there are two preferential directions for the veins one with strike to the SE and another with strike to the NE.*



*Figure 14 Sharp contact between shale and hydrothermally altered shale. The miners follow this contact in order to explore and exploit the emeralds.*

The shale that is not hydrothermally altered generally has a N-E course with dips of up to 85 ° SE.

The mine evidences a strong tectonic influence since the rock is highly fractured and filled with the mineralizing fluid which, through its high temperature and its highly oxidizing nature carbonitized and albitized the shale throughout the mine (Figs. 15 & 16). The hydrothermal fluid appears to have been multi-phase which are evident in stages of hydraulic breccia affecting previous veins (Fig. 17), the carbonate in its non-productive part presents a fibrous habit, while the emeralds crystallize in rhombohedral carbonates.

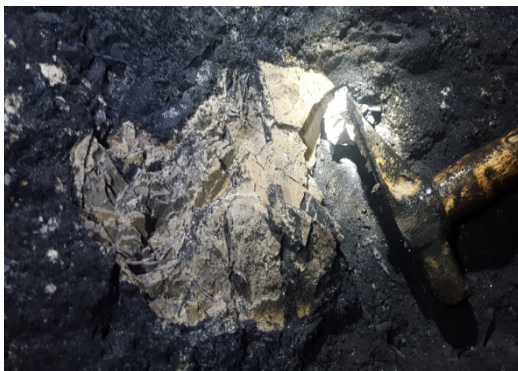


*Figure 15 Albitized shale due to the metasomatism of the rock.*



*Figure 16 Vein of carbonate deformed plastically by effect of compression and high temperatures.*



*Figure 17 Hydraulic brecciation due to the pressure released by the fluid.*

### **5.2.1.1 Microscopic observation**

The rocks, veins and rock-vein contacts show similar patterns which were previously described for the macroscopic observations. Below follows a brief description of representative samples from the mine.

**Sample 16:** The sample was taken from a non-productive vein in the Trapiche Tunnel which is 20 meters below the surface. The carbonates have suffered high deformation (Fig. 18). The carbonate in the photo shows a lamellae bent twinning resulting from the compressive tectonics, next to the bent carbonate there is a younger carbonate which has not been deformed. The carbonates do not show rhombohedral habit.

**Sample 15:** The sample was taken from Trapiche Tunnel and it is a vein in contact with the black shale (Figure 19). The black spot is organic matter which come from the shale. The thin section shows microcrystalline quartz surrounding the shale, where the highest temperatures are after hydraulic breccia. The closer the vein is to shale the greater the proportion of quartz, the more distant the temperature decreases and the more the proportion of carbonates and plagioclase (albite).



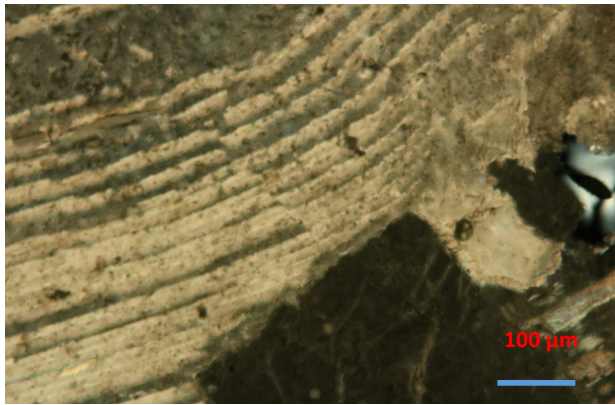


*Figure 18 Banded twinning due to deformation.*

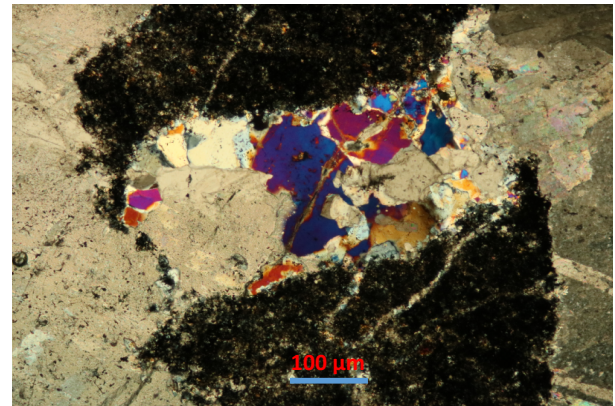


*Figure 19 Quartz and carbonate vein in contact with the black shale.*

#### 4.2.2 CUNAS

Cunas is south of the neighboring La Pita mine. It was discovered more than 25 years ago. It is nowadays not only one of the most productive mines in Colombia but also one of the most mechanized with wide tunnels, multiple powerful winches, modern security systems and above all, with an important social conscience that protects its workforce.

In a geological context, it shares very similar characteristics with La Pita. In Cunas, the main development direction follows the course of the Muzo Fault which juxtaposes fault blocks of the Muzo Formation. The great difference is that the hydrothermally altered shale are less common, but folds and veins are more frequent. It seems that the hydrothermal effect is not as intense as in La Pita, but the structures are more evident, recumbent and asymmetrical folds are found throughout the mine. The veins of carbonate, quartz and plagioclase cut the host rock without any preferential orientation. The size of the veins is relative and quite changeable (Fig. 20). There are veins of more than 50 cm width

which feed secondary veins of smaller size; this type of veins are called ‘cross fractures’. As in La Pita, there are sulfides such as pyrite and chalcopyrite.

The rocks do not have a well-defined strike because of the presence of many folds, many of which are tight and asymmetrical. However, in places where the rock is not so folded, it was possible to calculate a preferred structural trend of N50E / 83SE. N75E / 88SE for the black shale.

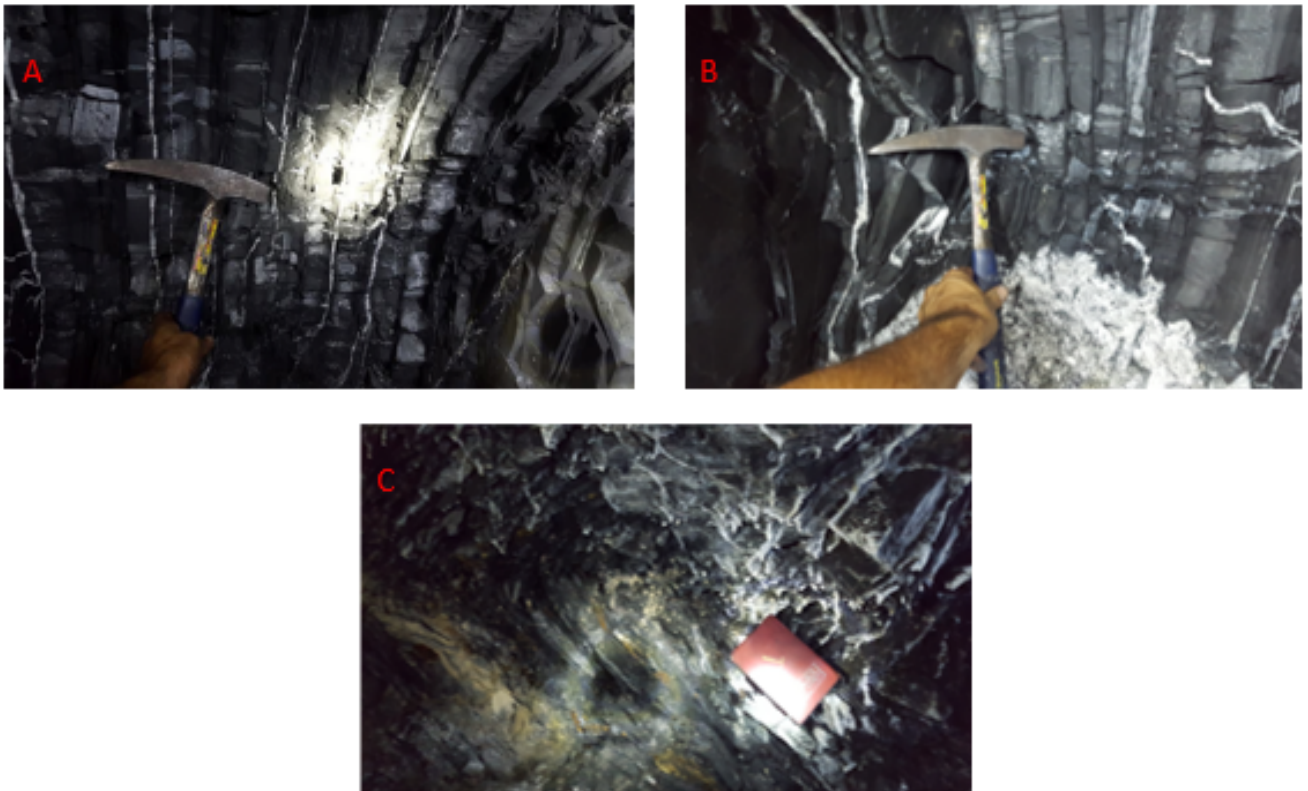


*Figure 20 Veins of carbonate following the shale foliation. The shale has an inclination close to 90 ° which shows the importance of the tectonic influence B. Cross veins cutting the shale with any preference direction C. Shale forming an anticline and subsequently affected by hydrothermal breccia.*

#### 4.2.2.1 Microscopic observation

**Sample 36:** The sample was taken from a productive vein that was in a hydraulic breccia. For this reason it is possible to find clasts of the shale in contact with the mineralizing vein. In the shale, it is possible to distinguish quartz clasts and plagioclase as a product of the hydrothermal alteration. In direct contact with the shale are the mineralizations of plagioclase (albite) which presents polysynthetic twinning and the quartz which has oblique extension due to the pressure on the mineral. Further away from the shale and in contact with the quartz-plagioclase is the carbonate which shows an obvious oxidation in the near surface environment (Fig. 21).

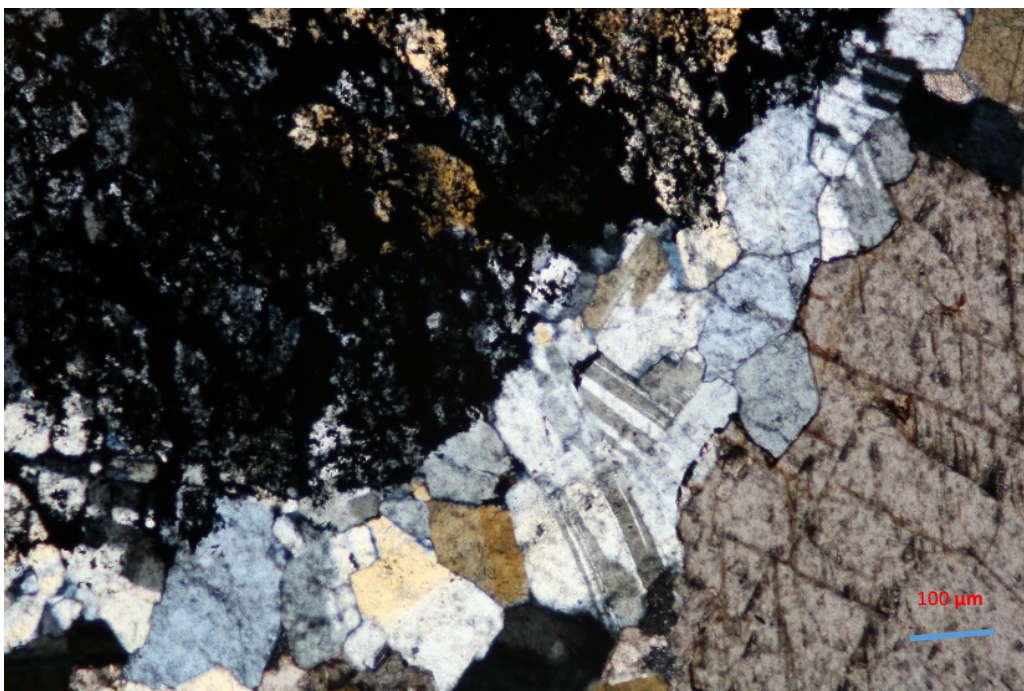


*Figure 21 Sample 32 showing the contact between the shale and the mineralization vein. Quartz and plagioclase mineralized next to the shale while the carbonate is further. Xpl.*



**Sample 37:** The sample was taken from a productive vein. It is evident that the early carbonate was subsequently brecciated by hydraulic pressure and plagioclase clasts with Carlsbad twinning were embedded in the carbonate which shows Lamella twinning (Fig. 22).

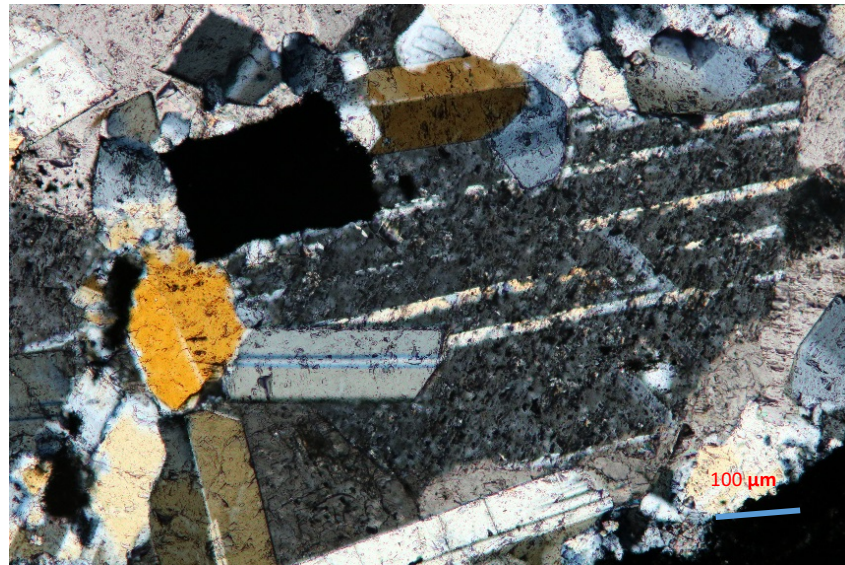


*Figure 22 Hydraulic Breccia in a productive vein from Cunas. Xpl.*

#### 4.2.3 ESPAÑOLES

This emerald mine is in the southernmost part of group 2. Like La Pita and Cunas, this mine is being explored on the slopes of the Minero River, assuming that the Rio Minero Fault trace follows the river bed.

The mine is in a very early stage of development because the investment has been limited and work has been sporadic. In terms of geology, the mine shows different characteristics to those seen in the other two mines of this group. The hydrothermal breccia of the host rock is not easily identifiable.

However, the rock is completely faulted and folded and subsequently suffered intense hydraulic

brecciation (Fig 23). Apparently, the mine is near the hinge of a large anticline. Fluid temperature and pressure within the partially crystallized veins may have been augmented during the folding episode and this may have generated cavities by explosive pressure release. The veins cut the shale and generated a chaotic structure (Fig. 24). The cavities were later filled by the fluid which was not enough to fill them, therefore carbonate geodes were formed, and within these geodes there was sufficient space for emeralds to crystallize.

For this reason, it is assumed that the mineralisation is controlled by hydraulic but not hydrothermal breccia, however the fluid was sufficiently reactive to leach the emerald, sulphide and carbonate forming elements from the shale to form the mineral associations (albite, quartz, emerald, pyrite chalcopyrite, etc.). Geodes were only noted in abundance in this mine and so are relevant to this comparative study.



*Figure 23 Hydraulic brecciation due high pression of the fluid in the rock.*



*Figure 24 Blocks of shale folded and severely fractured, the veins do not follow a preferred direction and are deformed plastically.*

The veins vary in thickness from centimetres to meters and cut the shale chaotically forming hydraulic breccias. The clasts are anhedral and irregular sizes. Most of the veins are plastically deformed (Fig. 24)

#### 4.2.3.1 Microscopic observation

**Sample 41:** The sample was taken from a productive vein in a hydraulic breccia. The presence of carbonate in different states is evident. Figure 25 shows two crystals of calcite that are not contemporary: an older phase is affected by the organic matter derived from the shale and a more recent phase contains clean carbonate with lamella twinning. Both this crystal, and a second-generation similar crystal, are fractured by the action of the same fluid.

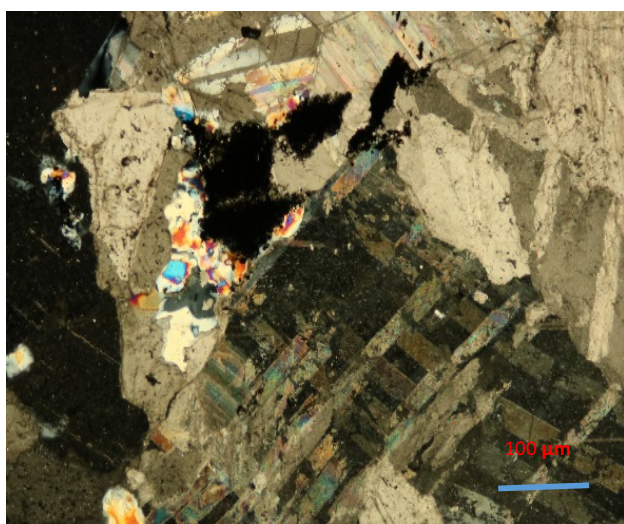


*Figure 25a multiple carbonate with a clast of shale embedded in one of them, quartz are surrounding the shale.*

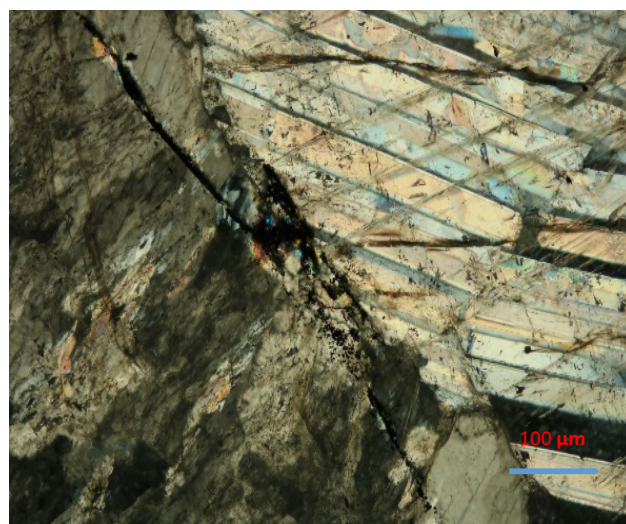
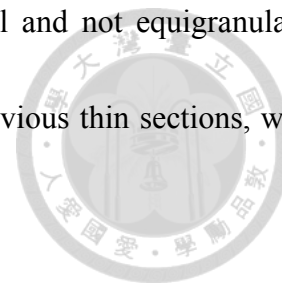


*Figure 25b Not contemporaneous carbonates in contact in a productive vein.*

In figure 24, several carbonates are in contact, the crystals are anhedral and not equigranular. A fragment of shale is embedded in one of the carbonates and, as in the previous thin sections, where shale is found there is quartz surrounding it.



### **4.3 GROUP 3**

#### **4.3.1 COSCUEZ**

More than a single mine, Coscuez is a sector in the WEB that has been exploited for hundreds of years by artisan miners. It is the most developed sector of the local economy. There are no mechanised techniques of any type and the mining is mainly done in small tunnels, which results in a high-risk environment for the miners.

The deposit is 10 km north of the Muzo deposit and is similar in its geological structural setting and paragenesis. According with previous authors, the area comprises two emerald-bearing vein-veinlet zones, which strike north-easterly and dip steeply. A second conjugate system of almost horizontal mineralized fractures is distinct (Kievlenko, 2003). However, this information could not be verified in our field trip since the visited zone were deposits of landslides.

The area visited is a site of debris flows on the slopes of a fairly steep hill with blocks up to 3 meters. This hill, like the others, have been excavated in a haphazard style without formal exploration studies (Fig. 26). It was possible to identify pyrite, carbonates and albite in the sector. However, a structural



study of this sector was not made since the available outcrops are not in situ. So, the collected samples were used for geochemical analysis.



*Figure 26 Artisanal mining in debris flows without any exploratory studies or mining safety.*

#### **5.3.1.1 Microscopic observation**

**Sample 30:** Sample taken from one of multiple veins that cut shale. This sample was selected to make thin sections as it perfectly shows the difference between two types of habit for calcite (Fig. 27). In the right side with a high birefringence is the fibrous calcite that suggests an early state of the emerald mineralization. This crystal has small particles of organic matter. On the left side is the orthorhombic carbonate with lamella twinning, which, on occasions can be associated with emerald.



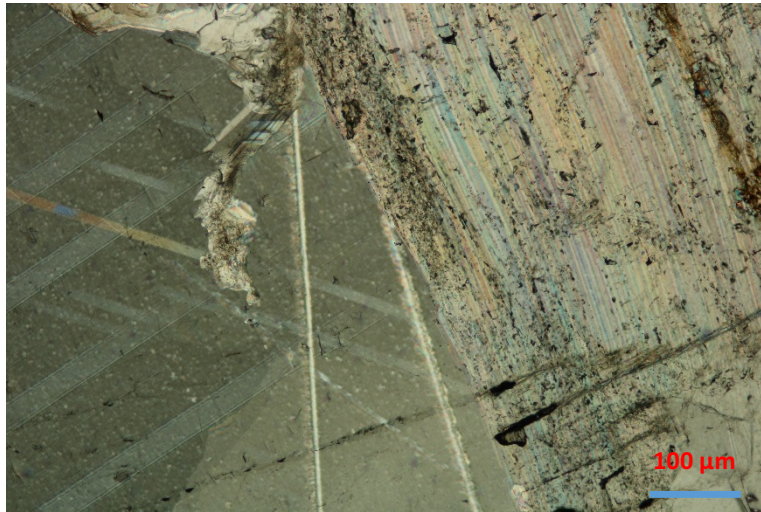


*Figure 27 Carbonates in contact with a plagioclase due the effect of hydraulic breccia.*

## 4.4 GROUP 4

### 4.4.1 MASATO AND PUERTO SIAD

Group 4 is located in the southernmost part of the study area and is located in the municipality of Muzo, which is the emerald capital of the world. It is perhaps the most famous sector for emeralds, particularly for large, high value stones. There are multiple mines, some more mechanised than others, plus many simple artisanal workings.

The mines visited in this sector were **Masato** and **Puerto Siad**. A separate study of both mines is not presented as they are very close geographically and they are exploited in the same hill, which, for the most part, is debris flow at the level of excavations (Fig. 28). Only one part of the Masato mine offered exposures of bedrock sedimentary formations, since the tunnel was about 800 meters in length.

The visit was limited for safety reasons, but in general there were some differences with the more northerly mines visited. The first and more visible was the lower proportion of pyrite and chalcopryrite

(Fig. 29). Nevertheless former sulphides are quite obvious in the oxidation environment. The population of veins is smaller, but the proportion of albite is greater compared to the mines previously visited. Both mines are in a very early stage of exploration and no gem quality emeralds have yet been found, only low quality ones which are known in the region as "gangas".



*Figure 28 Exploration in flow debris.*



*Figure 29 Higher oxidation in the shale because of the absent of pyrite and chalcoppyrite.*

#### **5.4.1.1 Microscopic observation**

**Sample 49:** The thin section shows different carbonates in contact. Carbonates have bend twinning by deformation. The replacement of carbonates by dissolution is clear. The youngest is fibrous while the one being replaced is orthorhombic, and due to the pressure, there is a crystal of plagioclase in the middle of the carbonates which has Carlsbad twinning (Fig. 30).

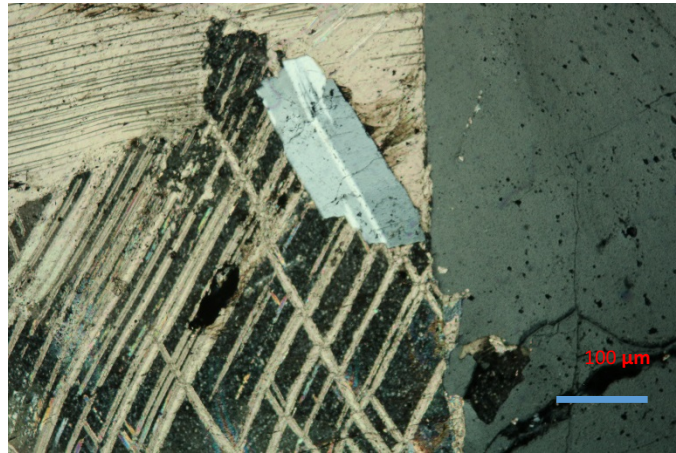


*Figure 30 Carbonates in contact with a plagioclase due the effect of hydraulic breccia.*

**Sample 54:** Sample taken at the contact between vein and shale in a hydraulic breccia. Within the shale and due to the fracturing of the same small veins are formed and are filled by microcrystalline quartz and plagioclase, the quartz presents waved extinction. The crystals are anhedral and irregular sizes (Fig.31).

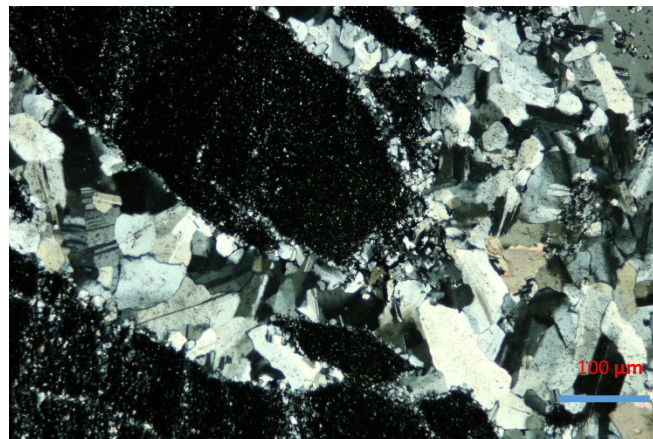
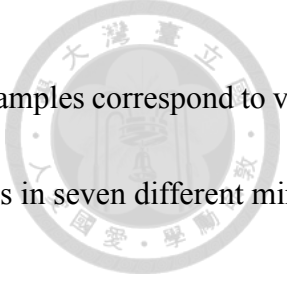


*Figure 31 Small veins in shale filled by microcrystalline quartz and plagioclase.*

## 5. MINERALOGY AND GEOCHEMISTRY

A total of 36 samples were selected for carbon and oxygen analyses. Those samples correspond to vein calcite, breccia and host rocks from the productive and non- productive areas in seven different mines from the WEB (Table 2). The separation of the samples was done manually.



Mine	# of samples
La Pita	17
Coscuez	3
Monteblanco	2
Cunas	3
Espanoles	7
Puerto Siad	2
Masato	3
Total	37

Table 2 Number of samples per mine.

The criteria for the classification of the samples according to their crystal habits, emerald potential zones and specific sample locations are set out below:

### *Crystal habit*

Three different calcite crystal habits were recognized:

1. *Fibrous calcite* (Fig. 32): According to Giullini 1994, this calcite is typical of the first stage of the emerald mineralization and is not associated directly with the emeralds since the beryl precipitated at a later stage. However, previous authors (Torres Giraldo, 2004) have reported emerald



mineralization in this stage, concluding that the fibrous calcite is indeed an early stage, but afterwards in a later recrystallization of the emeralds, the calcite is replaced. The emerald in this stage is not economically viable. Field observations for this research did not note emeralds in paragenesis with the fibrous calcite. The miners in the area do not recognize the fibrous calcite as a mineral indicator for the presence of emerald, therefore this crystal habit is interpreted as non-productive.



*Figure 32 Fibrous calcite.*

1. *Calcite Geode (Fig. 33)*: This occurrence was only found in Españoles mine. The reasons for geode hosted mineralization are: 1. The very complex structural geology in the mine, where more recent faults cut previous folds and faults plus steep dip angles for the stratigraphy of 75-85° in multiple orientations. Tight overturned, recumbent and asymmetrical anticlines are evident along the tunnels and galleries in Españoles. 2. The mine is probably located in the hinge of a large anticline where the pressure and temperatures are high enough to hydraulically

fracture the shale, and generate relatively large cavities. The mineralizing fluid is mobilized to these cavities, where pressure decreases lead to carbonate crystallization in a geode. 3. This calcite is assumed to be deposited in an intermediate stage, as the fibrous calcite is deposited in the absence of hydraulic breccia (Giulliani 1996). Emerald productivity in this setting is still debatable.



2.

*Figure 33 Calcite geode (taken from Torres Giraldo, 2004).*

2. *Rombohedral calcite (Fig. 34):* For emerald exploration, the rhombohedral calcite is a positive indicator, since this mineral is deposited in the latest stage for the emerald precipitation. Hydraulic breccias occur in high fluid-pressure zones related to stage 2 vein development (Giulliani 1996). This carbonate is present throughout the visited emerald mines and is a good proxy for emerald exploration. However, this proxy is not enough as not all the rhombohedral

carbonates are accompanied by green beryl. It is necessary to consider additional criteria in order to define a zone as a productive area.

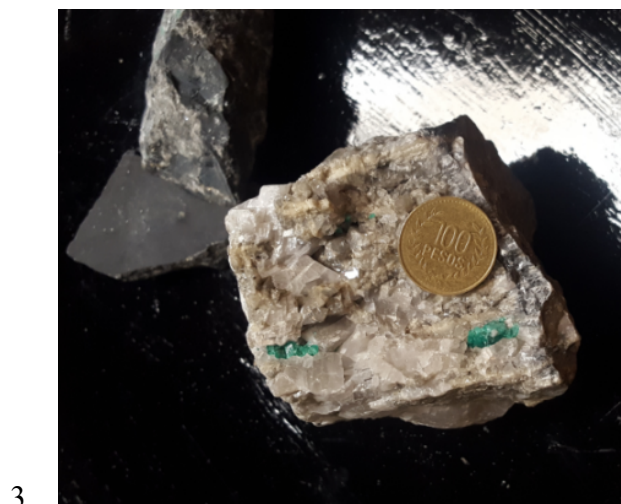


*Figure 34 Rhombohedral calcite with emerald*

#### *Emerald potential zones*

In the field, the emerald potential for each sample was determined on the basis of the parameters defined by Mantilla et al., 2007. These “indicators of reliability and risk”, would be a direct reflection of the degree of geological knowledge of the area of interest. The knowledge and experience of the miners are considered but sometimes these are not totally reliable since there are often contradictions between themselves.

The following are the field geological criteria to be considered to delimit areas with emerald potential (Modified from Mantilla et al., 2007).

1. *Depocenter area formed during the lower Cretaceous*: During the lower Cretaceous, this sector of the Colombian territory underwent a marine invasion of the Paleo-

Caribbean Sea, forming a bay (in a “back-arc” environment), whose southern limits extended approximately until the present Ecuadorian territory. In this paleogeographic context, there was an important accumulation of sediments, especially in the area of the aforementioned depocenter, where the WEB is now located.

All the sampled mines are located in this area

2. *Age of the rocks which host the hydrothermal manifestations:* Geological mapping with an important bio-stratigraphic component, made by INGEOMINAS (Reyes et al., 2006), has allowed the identification of two important belts, where the emeralds are hosted. In the WEB area, the emerald deposits are present in two formations: limestone of the Rosablanca Formation (Valanginian) and Shales of the Muzo Formation (Hauterivian-Barremian) with a thickness of approximately 160 to 300m.

All the sampled mines are in shales of the Muzo Formation.

3. *Tectonic and hydrothermal structures:* The emerald mineralization in the Muzo Formation located in the WEB is related with a very strong metasomatism of the black shales caused by the alkaline and saline fluid expelled by the compressive tectonics in the Paleogene. The fluid was driven by thrust faulting, and due to the pressure: hydraulic breccia, stockwork veins, geodes and hydrothermal breccias were developed. The shale shows albitization and carbonization which, in a later stage, is altered to kaolin. Tight recumbent, asymmetrical and overturned folds are common in the area.



4. *Mineralogical and geochemical aspects:* The emeralds in the WEB are in paragenesis with dolomite, ankerite, calcite and authigenic albite which precipitated after the interaction between the brines and the shale. Pyrite and chalcopyrite are not present everywhere but are important indicators for emeralds as those minerals represent sulphidation of the excess Fe available during the mineralising process, which limits the contamination and discolouration of the emeralds. The sulphides are precipitated due to the reduction of the fluid when it is in contact with the shale (Cheilletz et al., 1994). Quartz is also sometimes present, even forming druses. The presence of this mineral is assumed to be a result of an increase in the temperature within the hydrothermal system. All the mentioned minerals are emplaced in veins or breccia within the black shale. Some supergene minerals have been precipitated due to oxidation of primary minerals. Geochemical analyses in the electronic microscopy and RAMAN laboratory at the National Taiwan University identified: allophane  $\text{Al}_2\text{O}_3 \cdot (\text{SiO}_2)_{1.3-2} \cdot (2.5-3)\text{H}_2\text{O}$ , epsomite  $\text{MgSO}_4 \cdot 7\text{H}_2\text{O}$  and ettringite  $\text{Ca}_6\text{Al}_2(\text{SO}_4)_3(\text{OH})_{12} \cdot 26\text{H}_2\text{O}$  plus gypsum.
- All the foregoing minerals show the results of hydrothermal interaction between the host rocks and the brines and are positive indicators for emerald occurrence. All the mines show at least three of these minerals.
5. *Debris flow vs. Hydrothermal breccia:* The concept of hydrothermal breccia in the

shales can be confused with old debris flow zones. This characteristic is discussed for the first time in this research

In the study area, it is possible to recognize both hydrothermal breccia and secondary debris flow in the weathering zone using field criteria. The hydrothermal breccia generally manifests in very soft and carbonaceous altered shale, and it gives a non-compact appearance to the rock. Debris flows are most common in areas of high slope angles. Both deposits in the field can be confused by the miners. In the case of the Monteblanco mine, located at the base of a mountain, close to a river, it is evident that the miners are exploring debris flow deposits, since there is no continuity to the veins or faults. This contrasts with the situation at La Pita, developed in outcrop

For this reason, the Monteblanco, Puerto Siad and much of Masato mines are considered as relatively low probability productive areas as they are interpreted as being hosted in debris flow deposits. Any emeralds found around those mines is interpreted to be deposited from up slope via eluvial gravity slides.

The above primary characteristics for the exploration of emeralds. In some mines one feature may prevail over another and some characteristics may be absent. For example, in the La Pita mine the hydrothermal alteration is very evident and prevails, the shale is highly altered. However, in Españoles mine, the hydraulic breccia is dominant where the rock is highly fractured creating geodes. Both mines are productive.

For this research, the productivity factor is divided into three different categories: 1. Productive calcite (P), this includes all the samples that fulfil all or almost all the geological characteristics for a prolific area; some of the samples were picked in a proved emerald zone; 2. Non-productive area (Np): includes all of the samples that do not fulfil the minimum geological criteria for a prolific area. 3. Not defined area (Nd); includes all the samples that fulfil some of the geological criteria but not most of them.

The classification of the samples according to their crystal habit, emerald potential and where the samples were found are summarized in Table 3.

Sample	Mine	Calcite in (vein= v, Rock= r, breccia= b)	Crystal habit	Productivity (Productive= P. Nonproductive= Np, Not defined= Nd)
2	La Pita (Divino Niño)	v	Rombohedral	P
4	La Pita (Mecanizado 2)	v	Rombohedral	P
7	La Pita (Divino Niño)	v	Fibrous	Np
8	La Pita (Divino Niño)	v	Fibrous	Np
9	La Pita	v	Fibrous	Nd
10	La Pita	v	Fibrous	Nd
11	La Pita	v	Rombohedral	Nd
14	La Pita	v	Rombohedral	Nd
15	La Pita (Trapiche #1)	r	Fibrous	Np
16	La Pita (Trapiche #1)	v	Rombohedral	Nd
17	La Pita (Trapiche #2)	v	Rombohedral	P
18	La Pita (Trapiche #2)	v	Fibrous	Np
19	La Pita (Trapiche #2)	v	Rombohedral	P
23	La Pita (Nivel 3)	b	Rombohedral	Nd
26	La Pita (Trapiche 2)	v	Rombohedral	P
27	La Pita	r	Rombohedral	Nd
28	Coscuez	r	Fibrous	Nd
30	Coscuez	v	Fibrous	Nd
31	Coscuez	r	Rombohedral	Nd
32	Monteblanco	r	Fibrous	Np

33	Monteblanco	v	Fibrous	Np
35	Cunas	v	Rombohedral	p
36	Cunas	v	Rombohedral	p
37	Cunas	v	Rombohedral	p
38	Espanoles	v	Rombohedral	Nd
39	Espanoles	v	Fibrous	Nd
40	Espanoles	v	Fibrous	Nd
41	Espanoles	v	Rombohedral	P
43	Espanoles	r	Rombohedral	Nd
45	Espanoles	b	Geode	Nd
46	Espanoles	v	Rombohedral	Nd
49	Puerto Siad	v	Rombohedral	Np
51	Puerto Siad	b	Rombohedral	Np
54	Masato	b	Rombohedral	Nd
55	Masato	v	Rombohedral	Np
56	Masato	v	Fibrous	Np

Table 3 Classification of the samples selected for carbon and oxygen analysis.

### Analyses of stable isotopes of C and O

The study of the fractionation of stable isotopes was done mainly to understand the paleo-hydrogeological history of the study area, especially to main source of the fluid(s) which caused the emerald and associated mineralization (pyrite, calcite, chalcopryrite, quartz, albite, etc.). This is a fundamental tool to understand the physical and chemical changes of rocks and fluids, and in general to characterize these processes of fluid-rock interaction (Rollinson 1993).

The isotopic compositions were normalized to the Vienna Pee Dee Belemnite (V-PDB) for  $\delta^{13}\text{C}$  and

the Vienna Standard Mean Ocean Water (V-SMOW) for  $\delta^{18}\text{O}$  and  $\delta^{13}\text{C}$ . The  $\delta$  notation is defined as:

$\delta(\text{‰}) = [(R_{\text{sample}} / R_{\text{standard}}) - 1] \times 1000$ , where R is the ratio of either  $^{13}\text{C}/^{12}\text{C}$  or  $^{18}\text{O}/^{16}\text{O}$ . The

analytical precision (1s), based on replicate analyses of the carbonate standards, was 0.03 ‰ and 0.06

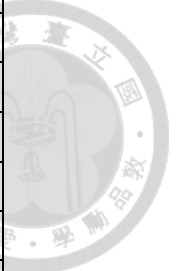
‰ for carbon and oxygen isotopes, respectively (Lu et al., 2017).

The  $\delta^{18}\text{O}$  and  $\delta^{13}\text{C}$  composition of the analyzed samples (in ‰), is presented in the Table 4. Using V-PDB and V-SMOW standards.

The following formula was used to convert the values from V-PDB to V-SMOW scale:

$^{18}\text{OVSMOW} = 1.03091 \times \delta^{18}\text{OVPDB} + 30.91 \text{ ‰}$  (Coplen 1988).

Sample Name	Mine	$\delta^{13}\text{C\_PDB}$ Mean (‰)	$\delta^{18}\text{O\_SMOW}$ Mean (‰)	$\delta^{18}\text{O\_PDB}$ Mean (‰)
2	La Pita	-3.99	22.72	-7.94
4	La Pita	-3.38	22.62	-8.04
7	La Pita	-4.80	23.29	-7.39
8	La Pita	-8.15	22.27	-8.38
9	La Pita	-5.34	22.88	-7.79
10	La Pita	-4.95	23.48	-7.21
11	La Pita	-5.90	23.16	-7.52
14	La Pita	-5.52	23.19	-7.49
15	La Pita	-6.64	21.17	-9.45
16	La Pita	-4.75	23.50	-7.19
17	La Pita	-5.09	23.33	-7.35
18	La Pita	-5.21	23.71	-6.99
19	La Pita	-5.38	22.64	-8.02
23	La Pita	-6.71	22.50	-8.16
26	La Pita	-5.73	22.73	-7.94
27	La Pita	-5.08	23.09	-7.58
28	Coscuez	-4.68	17.54	-12.97
30	Coscuez	-4.65	18.78	-11.76



31	Coscuez	-5.08	19.21	-11.35
32	Monteblanco	-7.49	17.80	-12.71
33	Monteblanco	-6.47	18.28	-12.25
35	Cunas	-1.86	22.98	-7.69
36	Cunas	-3.23	23.39	-7.30
37	Cunas	-4.06	22.80	-7.86
38	Espanoles	-2.82	23.69	-7.00
39	Espanoles	-4.68	22.90	-7.77
40	Espanoles	-3.41	22.95	-7.72
41	Espanoles	-3.27	22.28	-8.37
43	Espanoles	-5.42	20.01	-10.58
45	Espanoles	-2.75	20.83	-9.78
46	Espanoles	1.91	25.05	-5.68
49	Puerto Siad	-5.81	17.90	-12.62
51	Puerto Siad	-5.97	19.08	-11.47
54	Masato	-5.52	18.83	-11.72
55	Masato	-5.45	17.96	-12.57
56	Masato	-4.04	23.36	-7.33

*Table 4  $\delta^{18}\text{O}$  and  $\delta^{13}\text{C}$  composition of the analyzed samples for different mines (‰).*

For the  $\delta^{18}\text{O}$  composition of the measured samples the values ranged between 17.54 to 25.05‰ in V-SMOW standards. The data can be plotted in a diagram for natural oxygen reservoirs created by Rollinson in 1993. The values are very positive and suggest that magmatic reservoirs were not involved, instead suggesting sedimentary and metamorphic origins (Fig. 35).

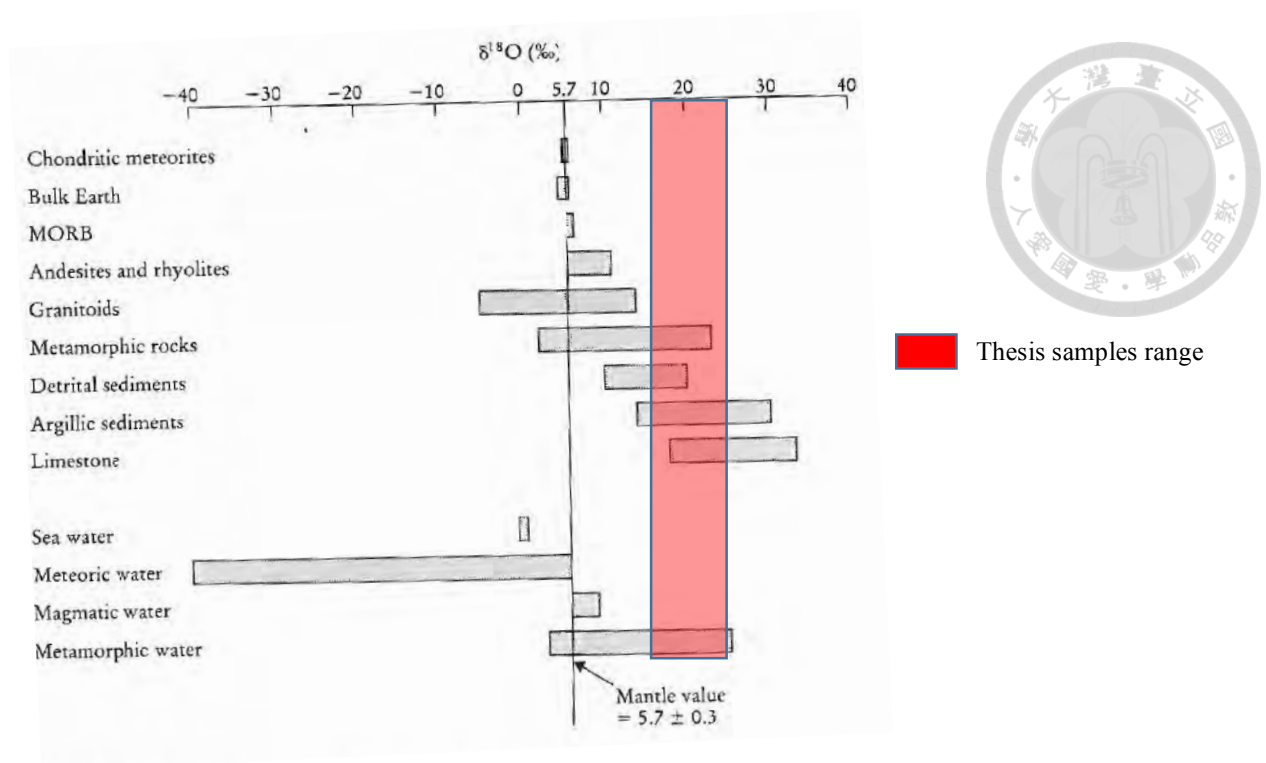


Figure 35 Natural Oxygen reservoir: Modified from Rollinson 1993.

The composition of  $\delta^{13}\text{C}$  for the same samples vary in a range between -7.49 to 1.91‰ in V-PDB standards. Rollinson 1993 also presented information from different authors to design a graph for natural oxygen reservoirs. The range for the samples from the WEB is plotted in Figure 36.

The fractionation of carbon isotopes is controlled by both equilibrium and kinetic processes. In many cases the fractionation of  $\delta^{13}\text{C}$  is strongly temperature dependant. But, dissolution and reprecipitation processes do not fractionate carbonates (Rollinson 1993).



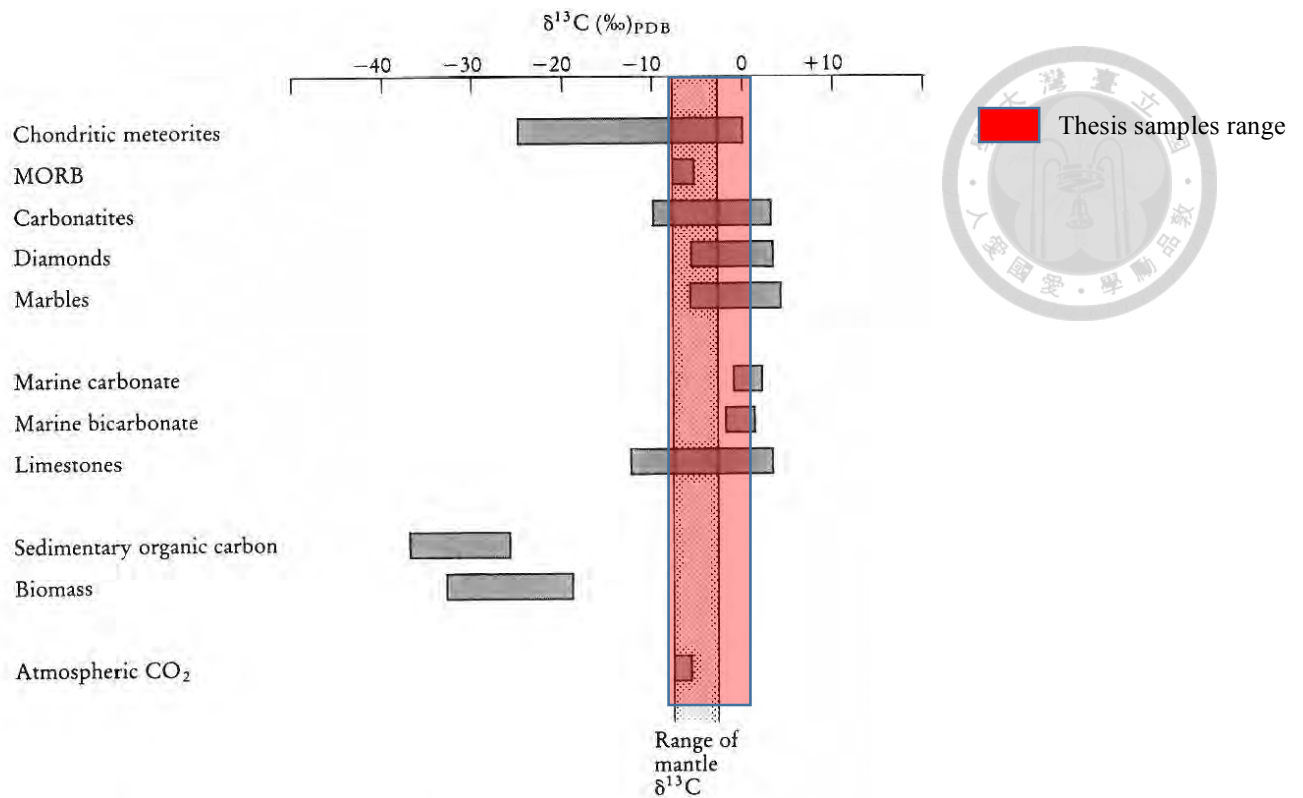


Figure 36 Natural Carbon reservoir. Modified from Rollinson 1993.

### Isotopic composition of H<sub>2</sub>O (δ<sup>18</sup>O<sub>H<sub>2</sub>O</sub>) and CO<sub>2</sub> (δ<sup>13</sup>C<sub>CO<sub>2</sub></sub>) in equilibrium with the calcites.

One of objectives of this study is to determine the original isotopic compositions of the fluids which mineralized the calcites. The resultant signature will help define the fluid character in a δ<sup>13</sup>C (PDB) vs δ<sup>18</sup>O (PDB – SMOW) diagram (Rollinson 1993). It is possible to calculate these parameters assuming different temperatures for the mineral formation. According to Cheilletz et al., 1994 and Mantilla, 2007 who studied primary fluid inclusions in calcites and emeralds, the temperature for emeralds formation is between 290- 360°C. Therefore, for the present research, in order to calculate the original isotopic composition of H<sub>2</sub>O and CO<sub>2</sub> in contact with calcites for the original fluid, the assumed temperatures

will be 290 °C, 315 °C, and 350°C and the different isotopic fractionation changes for the given temperatures are estimated.

The stable isotope fractionation calculation for H<sub>2</sub>O and CO<sub>2</sub> in contact with calcite was made using different formulas given by different authors. Below, detailed information explaining the procedure is presented. Simple programs to perform these calculations can be done directly on the following website: [http://www.ggl.ulaval.ca/cgibin/Isotope/generisotope\\_4alpha.cgi](http://www.ggl.ulaval.ca/cgibin/Isotope/generisotope_4alpha.cgi).

- *Stable Isotope Fractionation Calculation*

The isotopic composition of water ( $\delta^{18}\text{O}_{\text{H}_2\text{O}}$ ) in equilibrium with calcites was calculated using Kim, S.-T. & O'Neil, J.R. (1997) formula with temperatures between 25-350 °C:

$$1000 \ln \alpha = E \frac{(10^3)}{T} + F$$

**Equation: calcite $\rightleftharpoons$ H<sub>2</sub>O; T = 25-350 °C**

**E: 18.030; F: -32.420**

**T = 290 °C**

**1000 ln $\alpha$  = -0.4**

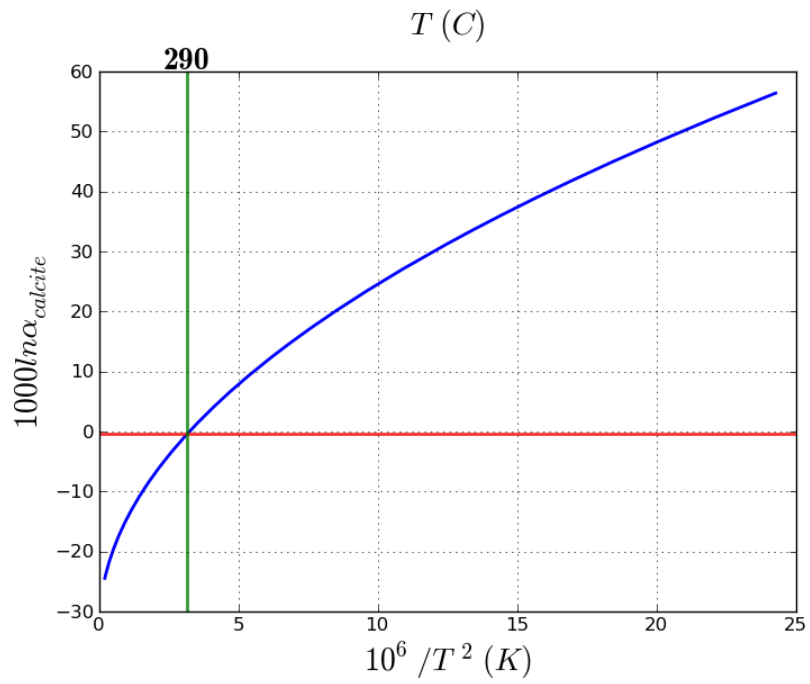


Figure 37  $1000 \ln \alpha = -0.4$  for  $T = 290^\circ\text{C}$ .

**$T = 320^\circ\text{C}$**

**$1000 \ln \alpha = -2.0$**

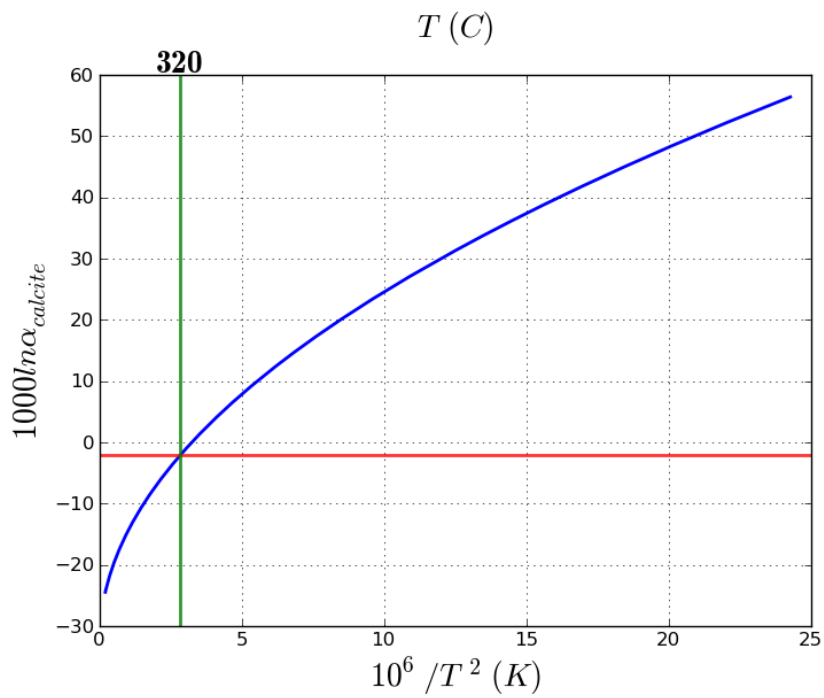


Figure 38  $1000 \ln \alpha = -2.0$  for  $T = 320^\circ\text{C}$ .

$$T = 350\text{ }^{\circ}\text{C}$$

$$1000 \ln \alpha = -3.5$$

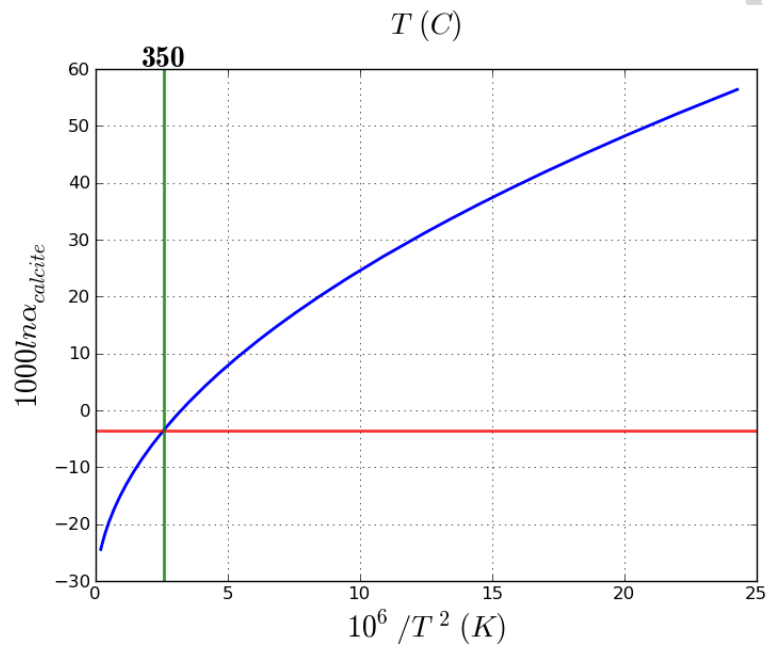


Figure 39  $1000 \ln \alpha = -3.5$  for  $T = 350\text{ }^{\circ}\text{C}$ .

The isotopic composition of Carbon dioxide ( $\delta^{13}\text{CCO}_2$ ) in equilibrium with calcites was calculated using Ohmoto y Rye (1976) formula with temperatures up to  $600\text{ }^{\circ}\text{C}$ :

$$1000 \ln \alpha = C \frac{(10^3)}{T^3} + D \frac{(10^6)}{T^2} + E \frac{(10^3)}{T} + F$$

Equation: calcite $\rightleftharpoons$ CO<sub>2</sub>;  $T < 600\text{ }^{\circ}\text{C}$

C: -0.8910; D: 8.557; E: -18.110; F: 8.270

$$1000 \ln \alpha = -1.9$$

$$T = 290\text{ }^{\circ}\text{C}$$

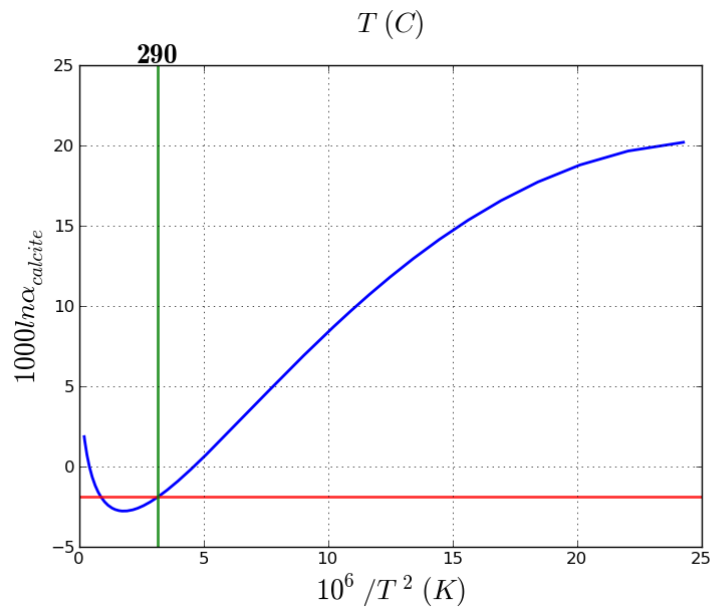


Figure 40  $1000 \ln \alpha = -1.9$  for  $T = 290^{\circ}C$ .

**$T = 320^{\circ}C$**

**$1000 \ln \alpha = -2.2$**

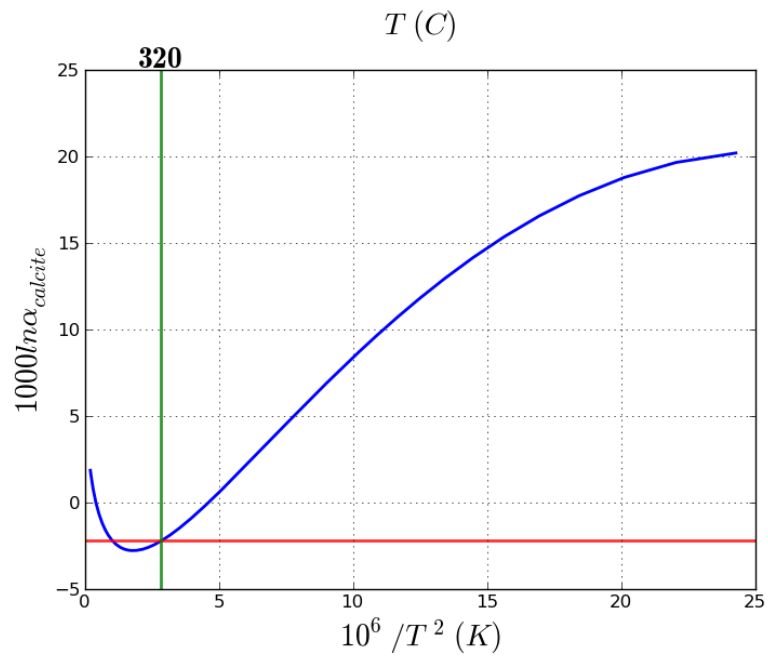


Figure 41  $1000 \ln \alpha = -2.2$  for  $T = 320^{\circ}C$ .

$$T = 350\text{ }^{\circ}\text{C}$$

$$1000 \ln \alpha = -2.4$$

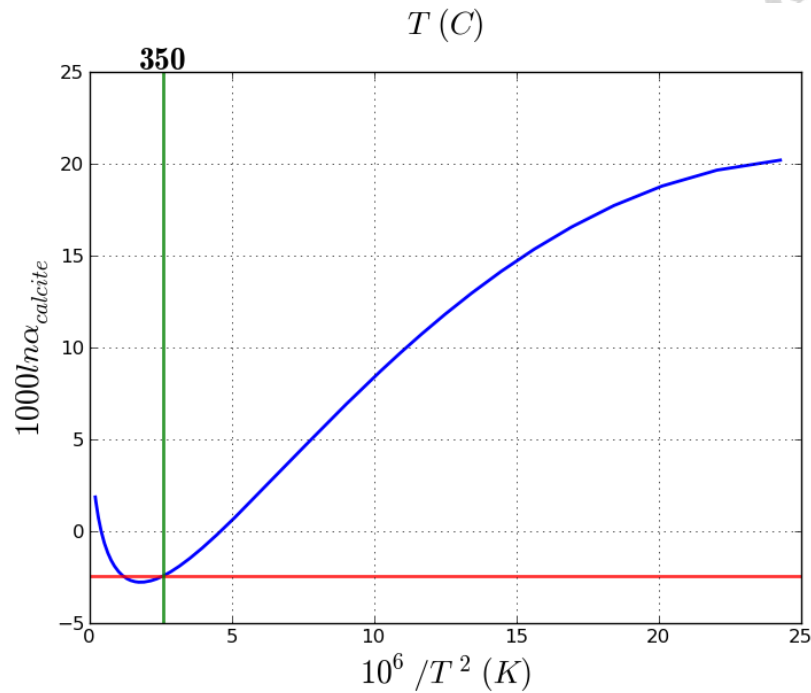


Figure 42  $1000 \ln \alpha = -2.4$  for  $T = 360\text{ }^{\circ}\text{C}$ .

After the stable isotope fractionation calculation for  $\text{H}_2\text{O}$  and  $\text{CO}_2$  in contact with calcite, it is possible to estimate the original isotopic composition for each sample at different temperatures ( $290\text{ }^{\circ}\text{C}$ ,  $320\text{ }^{\circ}\text{C}$ , and  $350\text{ }^{\circ}\text{C}$ ). The isotopic composition values of  $\text{H}_2\text{O}$  and  $\text{CO}_2$  in equilibrium with the calcites for each mine are summarized and represented in different tables and figures; providing an understanding of the changes in isotopic composition with temperature.

1. La Pita:

Sample Name	$\delta^{18}\text{O}_{\text{SMOW}}$ (ametur°C	$\delta^{18}\text{O}_{\text{SMOW}}$ (meture for	$\delta^{18}\text{O}_{\text{SMOW}}$ ((meture fo
2	22.32	20.72	19.22
4	22.22	20.62	19.12
7	22.89	21.29	19.79
8	21.87	20.27	18.77
9	22.48	20.88	19.38
10	23.08	21.48	19.98
11	22.76	21.16	19.66
14	22.79	21.19	19.69
15	20.77	19.17	17.67
16	23.10	21.50	20.00
17	22.93	21.33	19.83
18	23.31	21.71	20.21
19	22.24	20.64	19.14
23	22.10	20.50	19.00
26	22.33	20.73	19.23
27	22.69	21.09	19.59

*Table 5 Isotopic composition values of  $\text{H}_2\text{O}$  in equilibrium with calcites for La Pita at different T.*



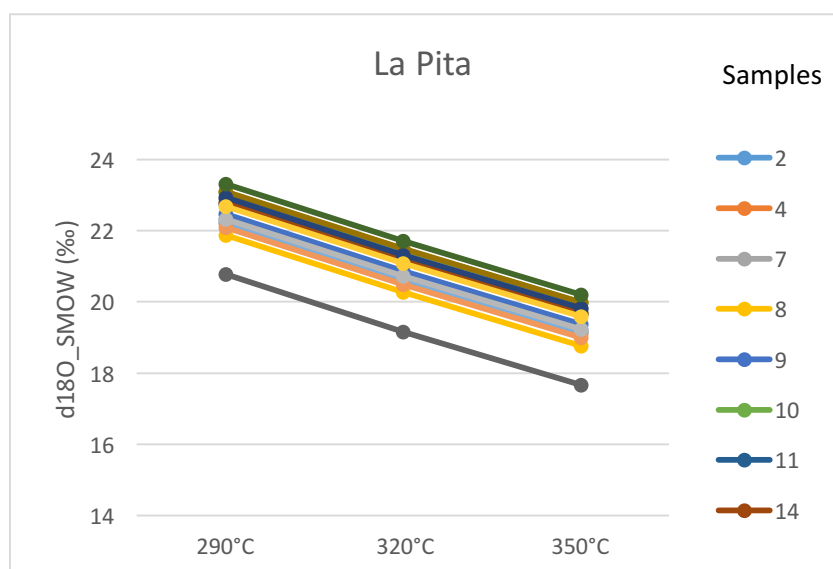


Figure 43 Isotopic composition of  $H_2O$  in equilibrium with calcites for La Pita at different  $T$ .

Sample name	$\delta^{13}C_{PDB}$ (namebrium)	$\delta^{13}C_{PDB}$ (n) (320B (	$\delta^{13}C_{PDB}$ (namebrium wit
2	-5.89	-6.19	-6.39
4	-5.28	-5.58	-5.78
7	-6.70	-7.00	-7.20
8	-10.05	-10.35	-10.55
9	-7.24	-7.54	-7.74
10	-6.85	-7.15	-7.35
11	-7.80	-8.10	-8.30
14	-7.42	-7.72	-7.92
15	-8.54	-8.84	-9.04
16	-6.65	-6.95	-7.15
17	-6.99	-7.29	-7.49
18	-7.11	-7.41	-7.61

19	-7.28	-7.58	-7.78
23	-8.61	-8.91	-9.11
26	-7.63	-7.93	-8.13
27	-6.98	-7.28	-7.48

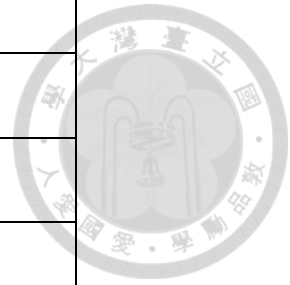


Table 6 Isotopic composition values of  $\text{CO}_2$  in equilibrium with calcites for La Pita at different  $T$ .

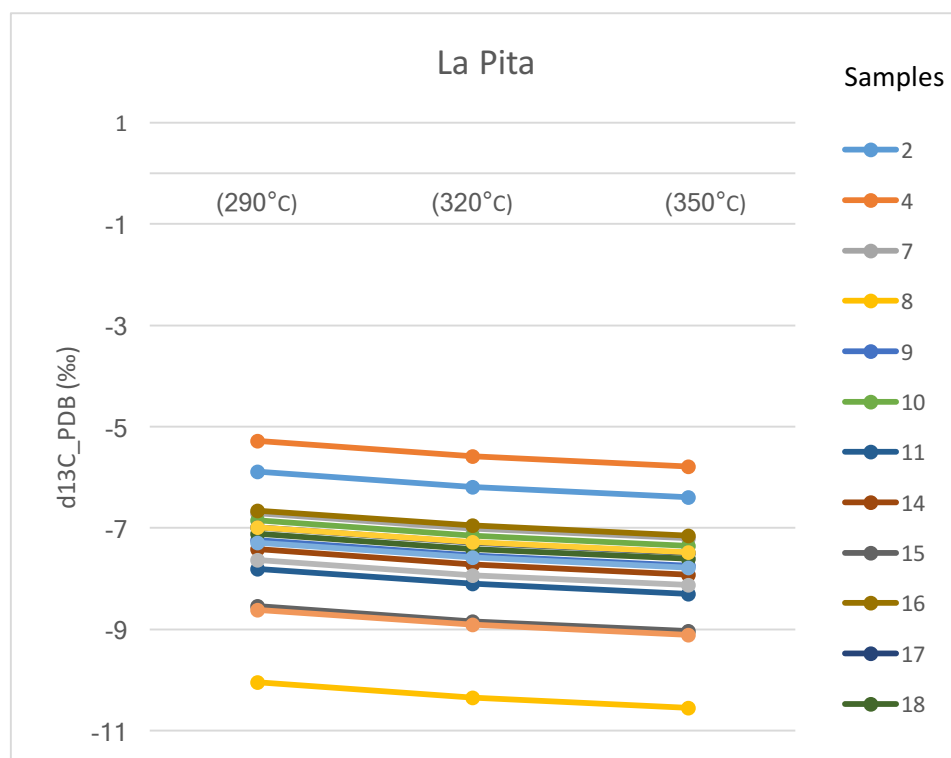


Figure 44 isotopic composition of  $\text{CO}_2$  in equilibrium with calcites for La Pita at different  $T$ .



## 2. Coscuez

Sample Name	$\delta^{18}\text{O}_{\text{SMOW}}$ (‰) 290°C	$\delta^{18}\text{O}_{\text{SMOW}}$ (‰) 290m wit	$\delta^{18}\text{O}_{\text{SMOW}}$ (‰) 290m wi
28	17.14	15.54	14.04
30	18.38	16.78	15.28
31	18.81	17.21	15.71

Table 7 isotopic composition values of  $\text{H}_2\text{O}$  in equilibrium with calcites for Coscuez at different  $T$ .

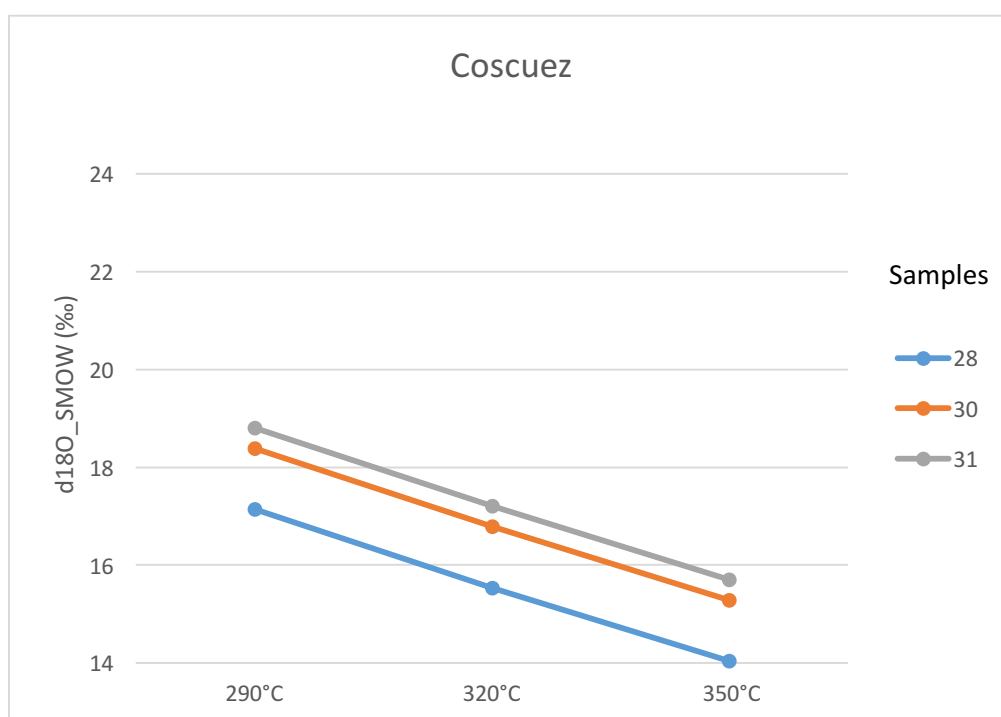


Figure 45 Isotopic composition of  $\text{H}_2\text{O}$  in equilibrium with calcites for Coscuez at different  $T$ .

Sample name	$\delta^{13}\text{C\_PDB}$ (namebrium	$\delta^{13}\text{C\_PDB}$ (namebrium	$\delta^{13}\text{C\_PDB}$ (namebrium wit
28	-6.58	-6.88	-7.08
30	-6.55	-6.85	-7.05
31	-6.98	-7.28	-7.48



Table 8 Isotopic composition values of  $\text{CO}_2$  in equilibrium with calcites for Coscuez at different  $T$ .

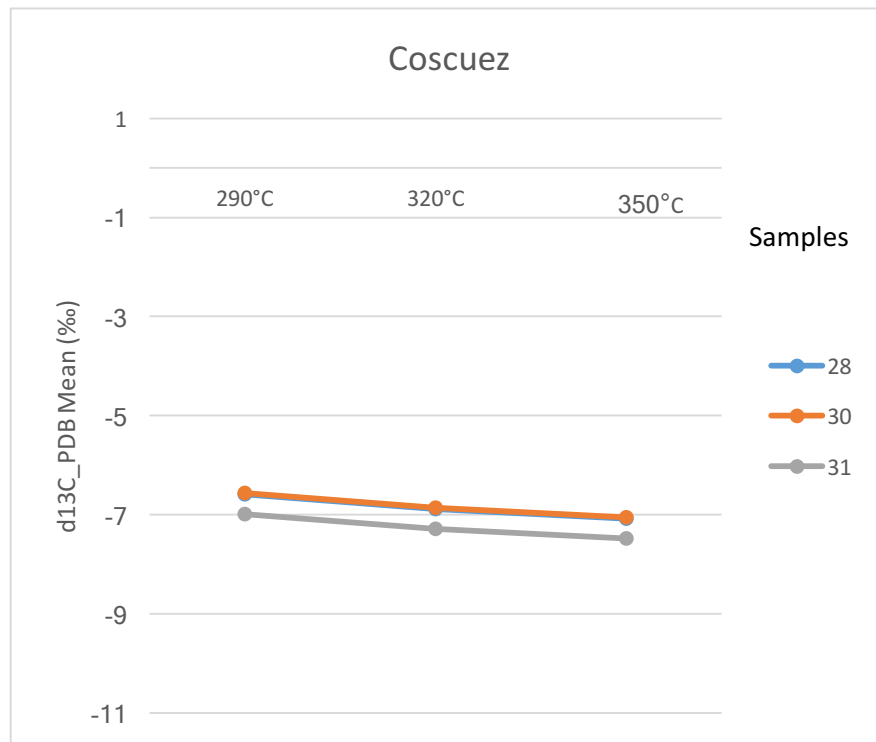


Figure 46 Isotopic composition of  $\text{CO}_2$  in equilibrium with calcites for Coscuez at different  $T$ .



## 1. Montebianco

Sample Name	$\delta^{13}\text{C}_{\text{PDB}}$ (‰) (290°C)	$\delta^{13}\text{C}_{\text{PDB}}$ (‰) (320°C)	$\delta^{13}\text{C}_{\text{PDB}}$ (‰) (350°C)
32	17.40	15.80	14.30
33	17.88	16.28	14.78

Table 9 Isotopic composition values of  $\text{H}_2\text{O}$  in equilibrium with calcites for Montebianco at different  $T$ .

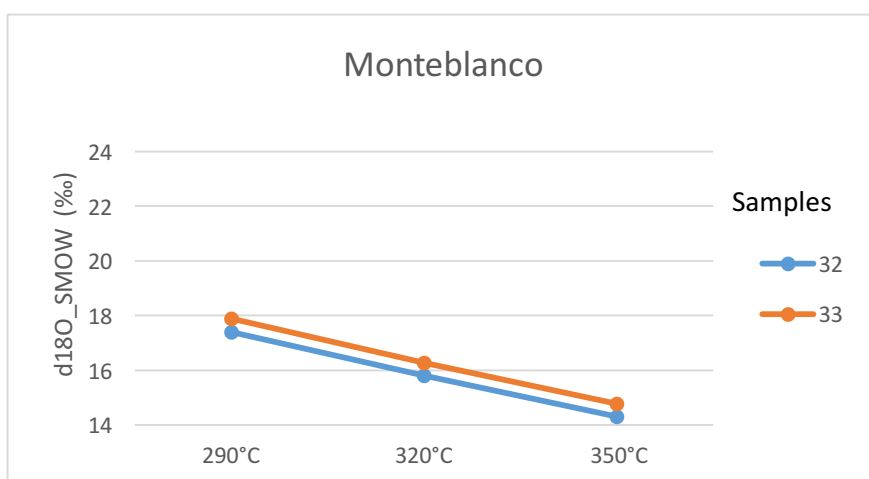


Figure 47 Isotopic composition of  $\text{H}_2\text{O}$  in equilibrium with calcites for Montebianco at different  $T$ .

Sample Name	$\delta^{13}\text{C}_{\text{PDB}}$ (‰) (290°C)	$\delta^{13}\text{C}_{\text{PDB}}$ (‰) (320°C)	$\delta^{13}\text{C}_{\text{PDB}}$ (‰) (350°C)
32	-9.39	-9.69	-9.89
33	-8.37	-8.67	-8.87

Table 10 Isotopic composition values of  $\text{CO}_2$  in equilibrium with calcites for Montebianco at different  $T$ .

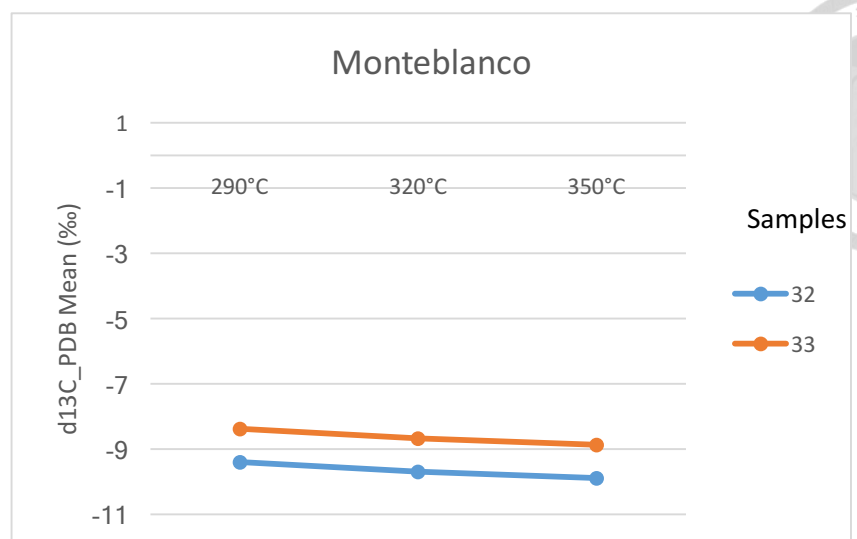


Figure 48 Isotopic composition of CO<sub>2</sub> in equilibrium with calcites for Monteblanco at different T.

## 2. Cunas

Sample Name	$\delta^{18}\text{O}_{\text{SMOW}}$ (290°C)	$\delta^{18}\text{O}_{\text{SMOW}}$ (_SMOW Name	$\delta^{18}\text{O}_{\text{SMOW}}$ (_SMOW Name
35	22.58	20.98	19.48
36	22.99	21.39	19.89
37	22.40	20.80	19.30

Table 11 Isotopic composition values of H<sub>2</sub>O in equilibrium with calcites for Cunas at different T.

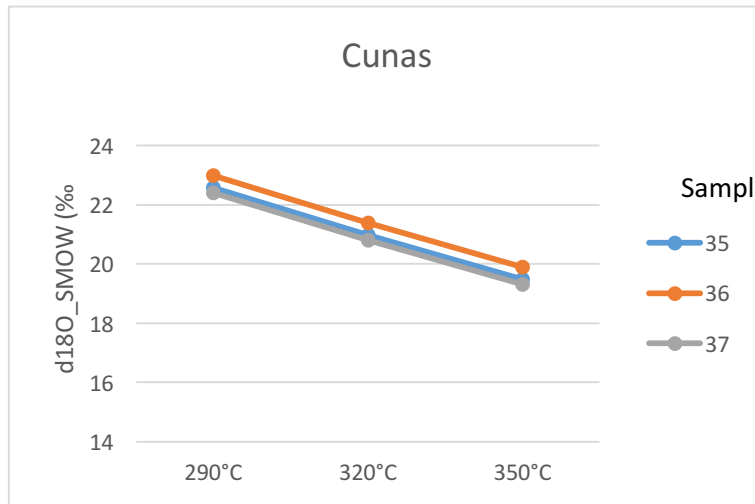


Figure 49 Isotopic composition of  $H_2O$  in equilibrium with calcites for Cunas at different  $T$ .

Sample name	$\delta^{13}C\_PDB$ (‰) (290°C)	$\delta^{13}C\_PDB$ (‰) (320°C)	$\delta^{13}C\_PDB$ (‰) (350°C)
35	-3.76	-4.06	-4.26
36	-5.13	-5.43	-5.63
37	-5.96	-6.26	-6.46

Table 12 Isotopic composition values of  $CO_2$  in equilibrium with calcites for Cunas at different  $T$ .

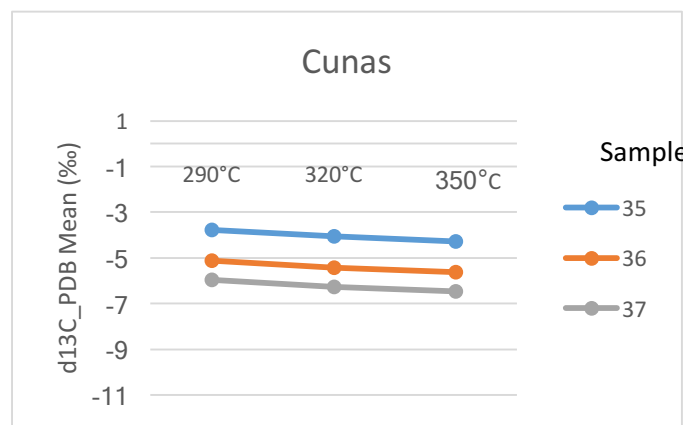


Figure 50 Isotopic composition of  $CO_2$  in equilibrium with calcites for Cunas at different  $T$ .



### 3. Españoles

Sample Name	$\delta^{18}\text{O}_{\text{SMOW}}$ (‰) (290°C)	$\delta^{18}\text{O}_{\text{SMOW}}$ (‰) (320°C)	$\delta^{18}\text{O}_{\text{SMOW}}$ (‰) (350°C)
38	23.29	21.69	20.19
39	22.50	20.90	19.40
40	22.55	20.95	19.45
41	21.88	20.28	18.78
43	19.61	18.01	16.51
45	20.43	18.83	17.33
46	24.65	23.05	21.55

Table 13 Isotopic composition values of  $\text{CO}_2$  in equilibrium with calcites for Españoles at different  $T$ .

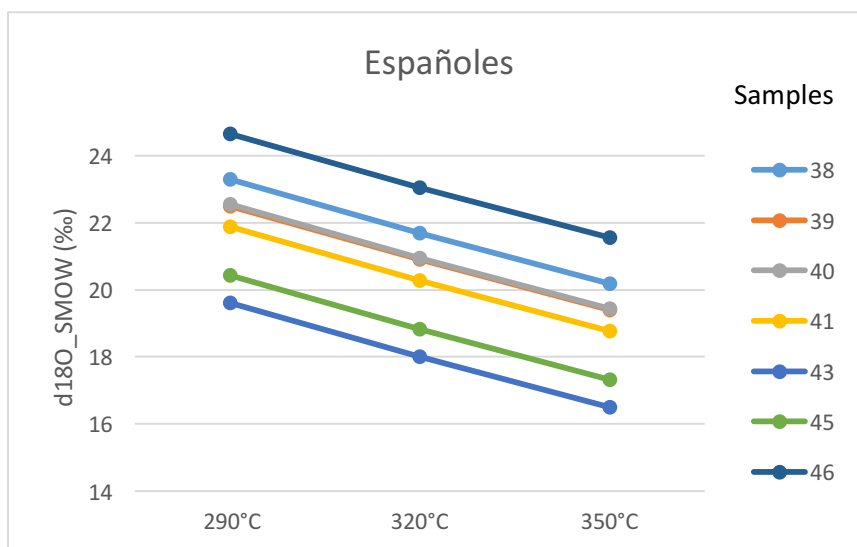


Figure 51 Isotopic composition of  $\text{H}_2\text{O}$  in equilibrium with calcites for Españoles at different  $T$ .

Sample name	$\delta^{13}\text{C\_PDB}$ (‰) (290°C)	$\delta^{13}\text{C\_PDB}$ (‰) (320°C)	$\delta^{13}\text{C\_PDB}$ (‰) (350°C)
38	-4.72	-5.02	-5.22
39	-6.58	-6.88	-7.08
40	-5.31	-5.61	-5.81
41	-5.17	-5.47	-5.67
43	-7.32	-7.62	-7.82
45	-4.65	-4.95	-5.15
46	0.01	-0.29	-0.49

Table 14 Isotopic composition values of  $\text{CO}_2$  in equilibrium with calcites for Españoles at different  $T$ .

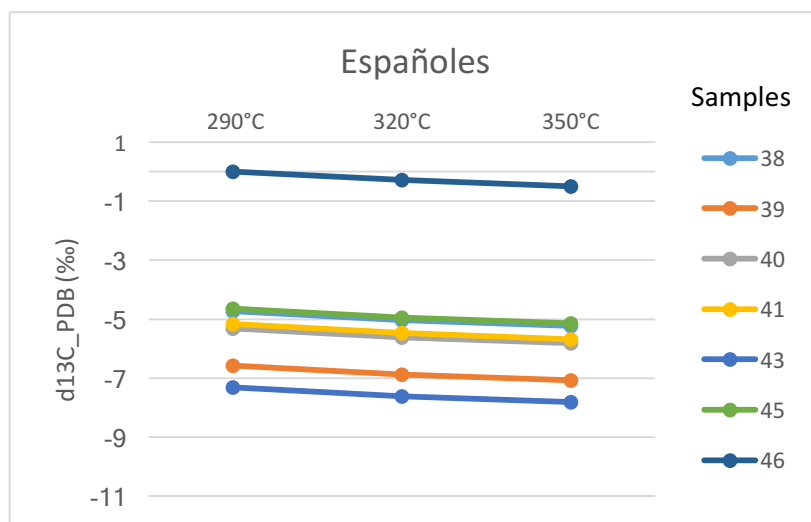


Figure 52 Isotopic composition of  $\text{CO}_2$  in equilibrium with calcites for Españoles at different  $T$ .

## 6. Puerto Siad

Sample Name	$\delta^{18}\text{O}_{\text{SMOW}}$ (‰) (290°C)	$\delta^{18}\text{O}_{\text{SMOW}}$ (‰) (320°C)	$\delta^{18}\text{O}_{\text{SMOW}}$ (‰) (350°C)
49	17.50	15.90	14.40
51	18.68	17.08	15.58



Table 15 Isotopic composition values of  $\text{H}_2\text{O}$  in equilibrium with calcites for Puerto Siad at different  $T$

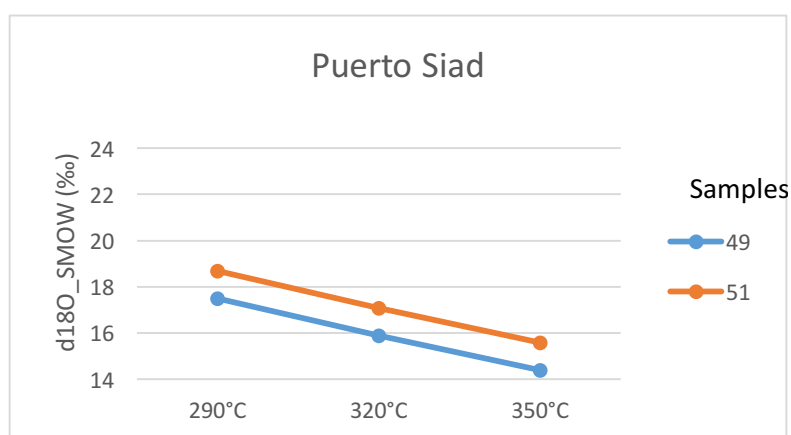


Figure 53 Isotopic composition of  $\text{H}_2\text{O}$  in equilibrium with calcites for Puerto Siad at different  $T$ .

Sample name	$\delta^{13}\text{C}_{\text{PDB}}$ (nament Tm	$\delta^{13}\text{C}_{\text{PDB}}$ (nament Tm	$\delta^{13}\text{C}_{\text{PDB}}$ (_PDB (nam
49	-7.71	-8.01	-8.21
51	-7.87	-8.17	-8.37

Table 16 Isotopic composition values of  $\text{CO}_2$  in equilibrium with calcites for Puerto Siad at different  $T$ .

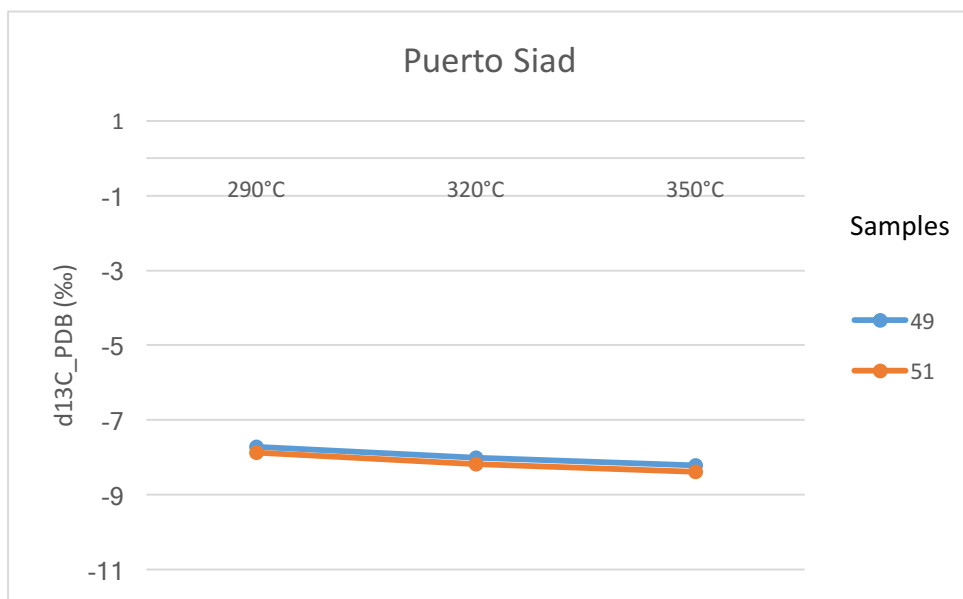


Figure 54 Isotopic composition of CO<sub>2</sub> in equilibrium with calcites for Puerto Siad at different T.

## 7. Masato

Sample Name	$\delta^{18}\text{O}_{\text{SMOW}}$ (ament T°C)	$\delta^{18}\text{O}_{\text{SMOW}}$ (_SMOW (ame	$\delta^{18}\text{O}_{\text{SMOW}}$ (ament T wi
54	18.43	16.83	15.33
55	17.56	15.96	14.46
56	22.96	21.36	19.86

Table 17 Isotopic composition values of H<sub>2</sub>O in equilibrium with calcites for Masato at different T.

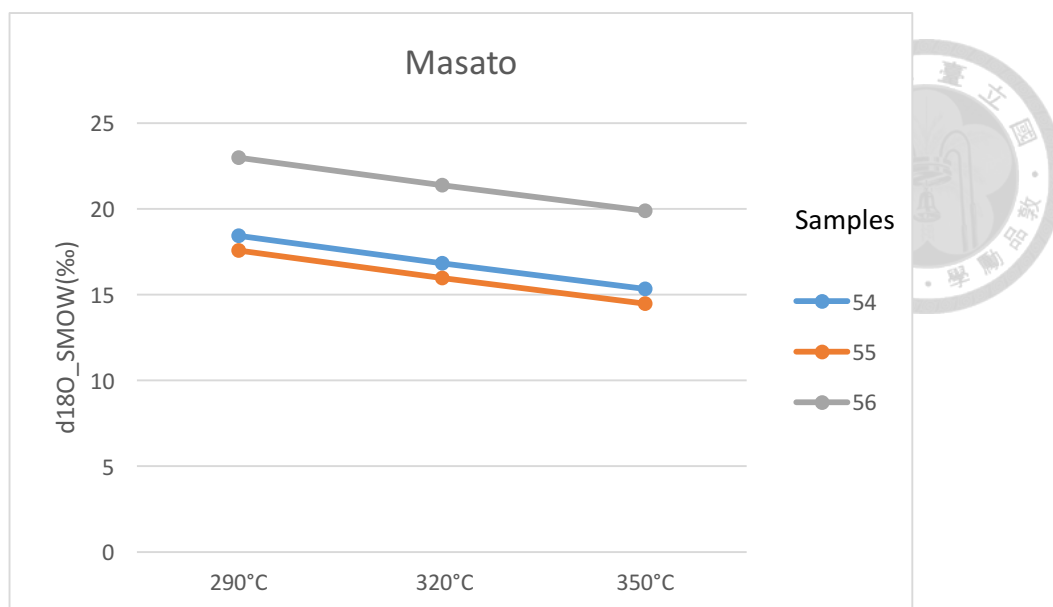


Figure 55 Isotopic composition values of  $\text{CO}_2$  in equilibrium with calcites for Puerto Said at different  $T$ .

Sample name	$\delta^{13}\text{C}_{\text{PDB}}$ (na (290B (	$\delta^{13}\text{C}_{\text{PDB}}$ (nament T w	$\delta^{13}\text{C}_{\text{PDB}}$ (nament T w
54	-7.42	-7.72	-7.92
55	-7.35	-7.65	-7.85
56	-5.94	-6.24	-6.44

Table 18 Isotopic composition of  $\text{CO}_2$  in equilibrium with calcites for Masato at different  $T$ .

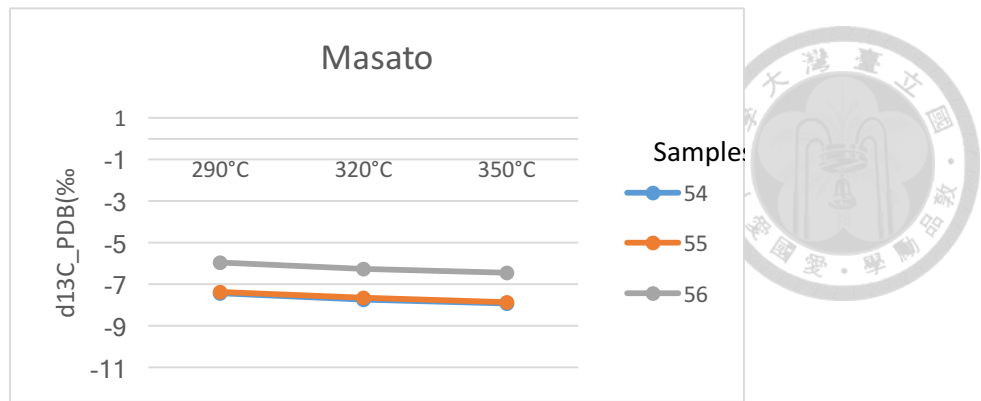


Figure 56 Isotopic composition of CO<sub>2</sub> in equilibrium with calcites for Masato at different T.

## 7. DISCUSSION AND CONCLUSIONS

For a better understanding and comprehension of the  $\delta^{13}\text{C}$  and  $\delta^{18}\text{O}$  behavior for each sampled mine within the WEB, a  $\delta^{13}\text{C}$  (PDB) vs.  $\delta^{18}\text{O}$  (SMOW) graph was drawn in order to summarize and plot the result. The reference temperature is 320°C since it is an intermediate measured temperature for the mineralization of emeralds (Fig. 57).

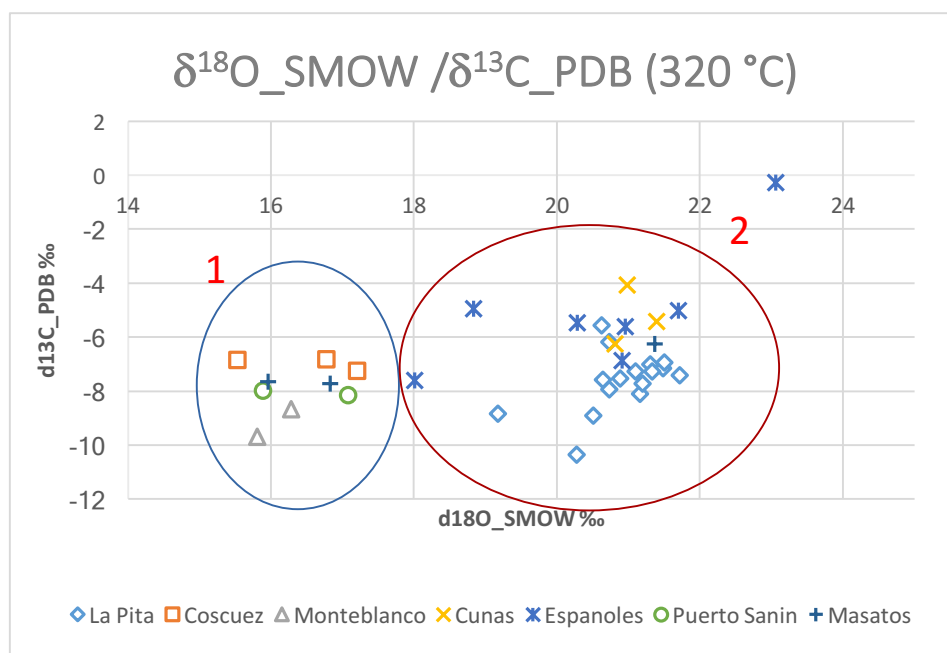


Figure 57  $\delta^{18}\text{O\_SMOW} / \delta^{13}\text{C\_PDB}$  at 320 °C for each sample in all the sampled mines.





According to the graph, we can group the results into two clusters:

1. Coscuez, 2 samples of Masato, Monteblanco and Puerto Siad: The range of  $\delta^{18}\text{O}$  SMOW is 15.8 to 17.6 ‰ and -6.5 to -9.8 for  $\delta^{13}\text{C}$ \_PDB
2. La Pita, Cunas, Españoles and a sample of Masato: The range of  $\delta^{18}\text{O}$  SMOW is 18 to 21.8 ‰ and -4 to -10.3 for  $\delta^{13}\text{C}$  PDB except for a sample of Españoles which presents values close to zero.

It is noteworthy that for the mines visited: those with the highest production history are La Pita and Cunas. In the field and as discussed above, La Pita, Cunas and Españoles are considered the most prospective, since they present hydrothermal alteration, thrust faults, folds, hydraulic breccia and a mineralogy which is characteristic for the mineralization of Colombian emeralds. Masato, Puerto Siad, Monteblanco and the sector visited in Coscuez do not meet all these characteristics. It is assumed that the mining in Monteblanco, Puerto Siad and part of Masato is being done on old debris flow deposits. However, it should be noted that a sample of Masato is within group 1, which would be interesting to review for prospecting purposes.

The original isotopic composition of the samples for each mine were plotted in a diagram  $\delta^{13}\text{C}$  (PDB) vs.  $\delta^{18}\text{O}$  (SMOW) (Rollinson, 1996) which shows the isotopic composition of a number of different carbonate reservoirs. Figures 58.

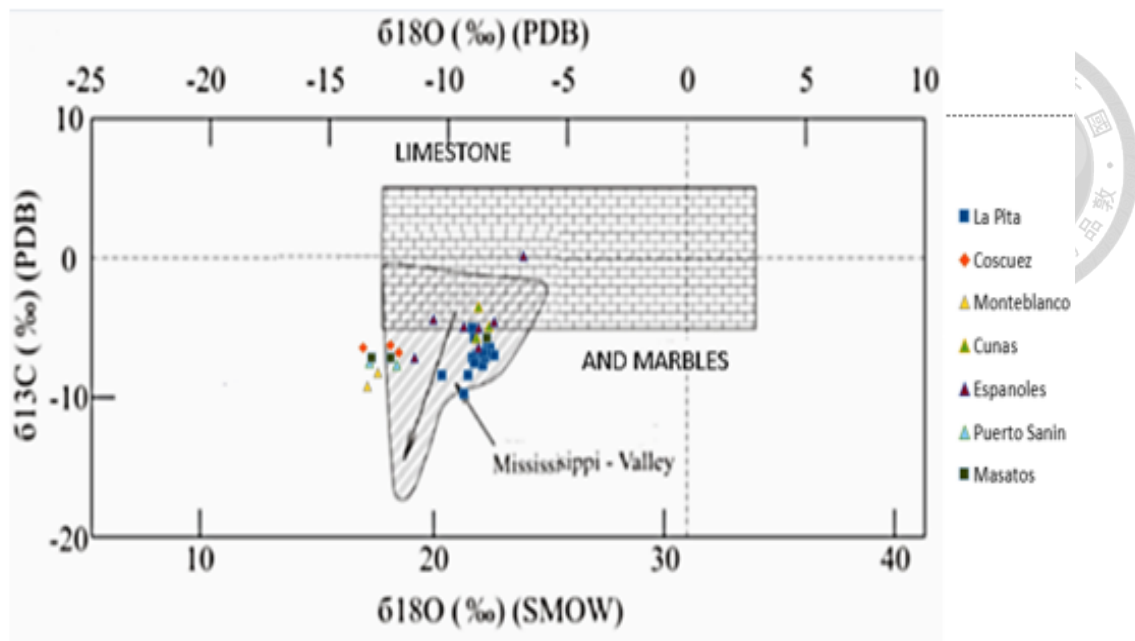


Figure 58 Isotopic composition of a number of different carbonate reservoirs for WEB mines samples at 290°C. Modified from Rollinson, 1993.

The calcites collected from seven different mines within the WEB are, according to the Figures 58, comparable with those fluids forming Mississippi Valley-Type (Pb-Zn) deposits. These are hydrothermal sedimentary hosted deposits containing economically important deposits of lead, zinc and other elements including silver. However, by context the MVT deposition temperatures are of low temperature and do not exceed 200 ° C since they come from sedimentary sources that have undergone compaction, in the case of Colombian emerald deposits the temperatures are much higher (290 ° C- 360 ° C), and the reason for these high values is a subject that is still under discussion.

According to Figures 58, at all temperatures, samples belonging to La Pita, Cunas and Españoles (i.e. those mines producing more emeralds) are in the calcite, marble and Mississippi Valley Type deposit

area, which supports the idea of a sedimentary and metamorphic origin for the mineralization. On the other hand, the other mines at a low temperature are located within or very close to the Mississippi Valley Type deposit zones. Only one sample (from Españoles) is located in the area of marbles, where tectonic influence is more evident than in any other mine. Tight folds, hydraulic breccia and associated faults generate veins and geodes that, through pressure alone, may have generated minor metamorphic effects.

The isotopic composition of a mineral formed in isotopic equilibrium with the aqueous medium, is a function of: the formation temperature, the isotopic composition of the water and the salinity of the fluid. The reasons to explain why there are two different clusters of results from WEB mines classified by  $\delta^{18}\text{O}$  and  $\delta^{13}\text{C}$  composition (Fig. 59) are explained below:

1. *The mineralizing fluid may be common* but may reflect two different stages of evolution within the WEB. For group 1, which has lower values for  $\delta^{18}\text{O}$ , the fluid is at an earlier stage where the isotopic exchange between rock and fluid is less complete than for group 2. For group 2 the fluid is more mature and has reacted more thoroughly with the shale which would allow a more intense leaching of reactive elements from the host rock. Negative values for  $\delta^{13}\text{C}$  are a response of the oxidation in the system suffered by the  $\text{SO}_4^{2-}$ ,  $\text{NO}_3^-$  and  $\text{BO}_3^-$  from the brines (Giulliani, 2017).
2. *Alternatively, there are two mineralizing fluids* involved in the precipitation of carbonates in the WEB. One is lighter in  $\delta^{18}\text{O}$  composition and is not reactive enough to leach all the emerald

forming elements from the shales. While the fluid that mineralizes the carbonates of group 2 is heavier and more reactive, facilitating the precipitation of emeralds and other minerals.

It is interesting to note that for group 2 the composition of  $\delta^{13}\text{C}$  is more negative in the north of the WEB than in the south. In fact, a sample of Españoles is very close to 0 ‰ value. This may be because the shale has a more organic content in the south than in the north. Organic content may neutralize the oxidizing character of the brines. The shales in Españoles seem to have undergone a weak local metamorphic event which may have degraded organic matter. According to the productivity classification of each sample described in the Table 3, the productive and non-productive samples were plotted in a graph  $\delta^{18}\text{O}_{\text{SMOW}} / \delta^{13}\text{C}_{\text{PDB}}$  at 320 C (Fig. 60).

For exploration purposes: A range for  $\delta^{18}\text{O}$  (SMOW) between 18 to 21.8 ‰ and -4 to -10.3‰ for  $\delta^{13}\text{C}$  (PDB) represent the isotopic signature of the hydrothermal fluids which led the emerald mineralization for the visited mines. Therefore, any calcite coming from hydrothermal veins from the Muzo Formation in the WEB, with an isotopic value close to this range of values, and with the appropriate geological setting has the possibility of being associated with emeralds.

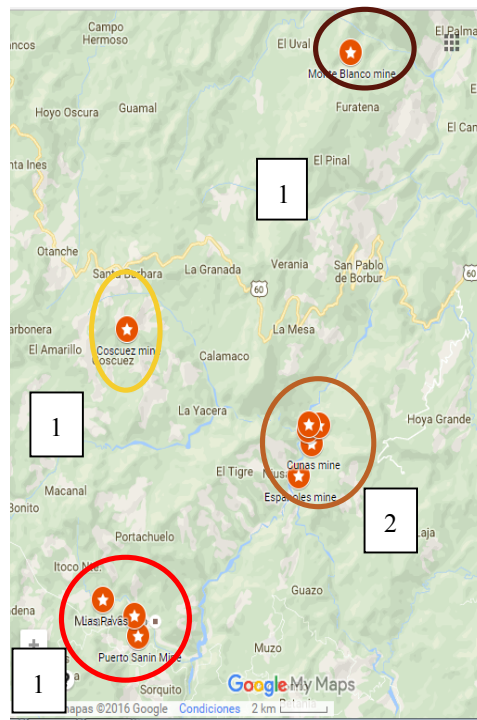


Figure 59. The two different groups of mines in the WEB classified by  $\delta^{18}\text{O}$  and  $\delta^{13}\text{C}$  composition

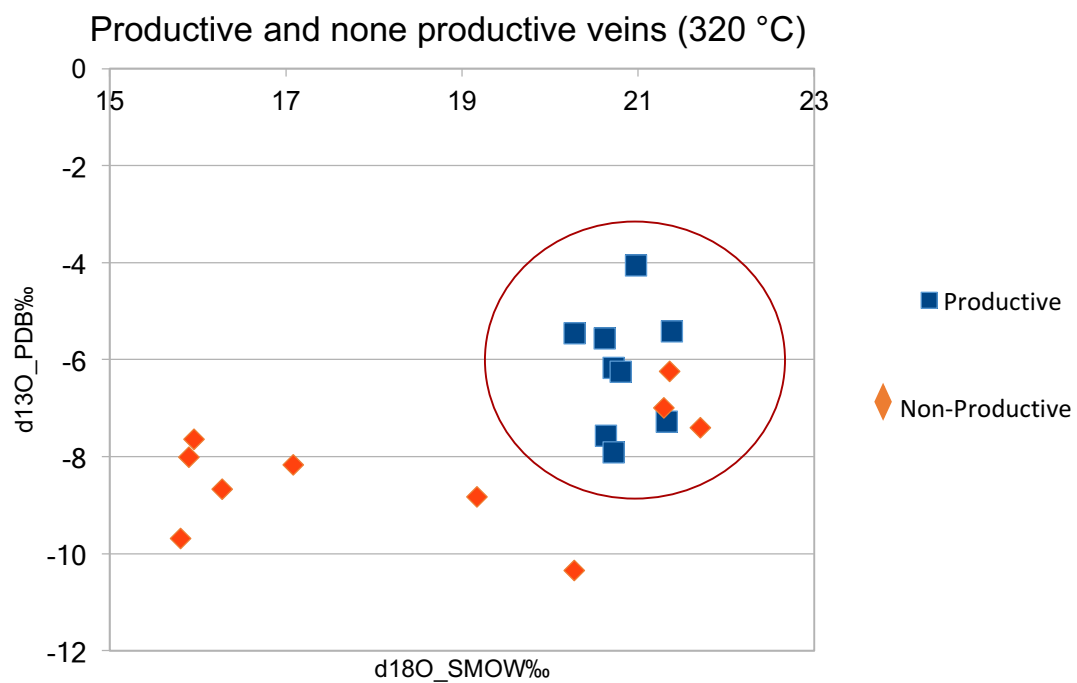


Figure 60. Productive and none-productive veins (320 °C) in the mines on the WEB.

## 8. REFERENCES

- Arif, M., Fallick, A. E., & Moon, C. J. (1996). The genesis of emeralds and their host rocks from Swat, northwestern Pakistan: a stable-isotope investigation. *Mineralium Deposita*, 31(4), 255-268. doi:10.1007/s001260050032
- Barton, M. D., & Young, S. (2002). Non-pegmatitic Deposits of Beryllium: Mineralogy, Geology, Phase Equilibria and Origin. *Reviews in Mineralogy and Geochemistry*, 50(1), 591-691. doi:10.2138/rmg.2002.50.14
- Bosshart, G. (1991). Emeralds from Colombia (Part 2). *The Journal of Gemmology*, 22(7), 409-425. doi:10.15506/jog.1991.22.7.409
- Bowersox, G., Snee, L. W., Foord, E. E., & Seal, R. R. (1991). Emeralds of the Panjshir Valley, Afghanistan. *Gems & Gemology*, 27(1), 26-39. doi:10.5741/gems.27.1.26
- Bozkaya, G., & Banks, D. A. (2015). Physico-chemical controls on ore deposition in the Arapucandere Pb–Zn–Cu-precious metal deposit, Biga Peninsula, NW Turkey. *Ore Geology Reviews*, 66, 65-81. doi:10.1016/j.oregeorev.2014.10.014
- Branquet, Y., Laumonier, B., Cheilletz, A., & Giuliani, G. (1999). Emeralds in the Eastern Cordillera of Colombia: Two tectonic settings for one mineralization. *Geology*, 27(7), 597. doi:10.1130/0091-7613(1999)027<0597:eiteco>2.3.co;2
- Cheilletz, A., Feraud, G., Giuliani, G., & Rodriguez, C. T. (1994). Time-pressure and temperature constraints on the formation of Colombian emeralds; an  $^{40}\text{Ar}/^{39}\text{Ar}$  laser



microprobe and fluid inclusion study. *Economic Geology*, 89(2), 361-380.  
doi:10.2113/gsecongeo.89.2.361

- Cheilietz, A., & Giuliani, G. (1996). The genesis of Colombian emeralds: a restatement. *Mineralium Deposita*, 31(5), 359-364. doi:10.1007/bf00189183
- Giuliani, G., France-Lanord, C., Zimmermann, J. L., Cheilietz, A., Arboleda, C., Charoy, B., . . . Giard, D. (1997). Fluid Composition,  $\delta D$  of Channel H<sub>2</sub>O, and  $\delta^{18}O$  of Lattice Oxygen in Beryls: Genetic Implications for Brazilian, Colombian, and Afghanistani Emerald Deposits. *International Geology Review*, 39(5), 400-424. doi:10.1080/00206819709465280
- Giuliani, G., France-Lanord, C., Coget, P., Schwarz, D., Cheilietz, A., Branquet, Y., . . . Piat, D. H. (1998). Oxygen isotope systematics of emerald: relevance for its origin and geological significance. *Mineralium Deposita*, 33(5), 513-519. doi:10.1007/s001260050166
- Giuliani, G., Cheilietz, A., Arboleda, C., Carrillo, V., Rueda, F., & Baker, J. H. (1995). An evaporitic origin of the parent brines of Colombian emeralds: fluid inclusion and sulphur isotope evidence. *European Journal of Mineralogy*, 7(1), 151-166. doi:10.1127/ejm/7/1/0151
- Giuliani, G., Dubessy, J., Ohnenstetter, D., Banks, D., Branquet, Y., Feneyrol, J., . . . Martelat, J. (2017). The role of evaporites in the formation of gems during metamorphism of carbonate platforms: a review. *Mineralium Deposita*. doi:10.1007/s00126-017-0738-4
- Henderson, P. (1994). *Rare earth element geochemistry*. Amsterdam: Elsevier.

- Horton, B. K., Saylor, J. E., Nie, J., Mora, A., Parra, M., Reyes-Harker, A., & Stockli, D. F. (2010). Linking sedimentation in the northern Andes to basement configuration, Mesozoic extension, and Cenozoic shortening: Evidence from detrital zircon U-Pb ages, Eastern Cordillera, Colombia. *Geological Society of America Bulletin*, 122(9-10), 1423-1442. doi:10.1130/b30118.1
- Keller, P. C. (1981). Emeralds of Colombia. *Gems & Gemology*, 17(2), 80-92. doi:10.5741/gems.17.2.80
- Keller, P. C. (1990). Hydrothermal Gem Deposits: The Emerald Deposits of Colombia. *Gemstones and Their Origins*, 39-55. doi:10.1007/978-1-4684-6674-4\_3
- “La Page Que Vous Cherchez N'est plus Disponible.” Faculté Des Sciences Et De Génie: Ce Que Vous Cherchez N'est plus Disponible, [www.ggl.ulaval.ca/cgibin/isotope/generisotop\\_4alpha.cgi](http://www.ggl.ulaval.ca/cgibin/isotope/generisotop_4alpha.cgi).
- Lu, Y., Song, S., Wang, P., Wu, C., Mii, H., Macdonald, J., John, C. M. (2017). Magmatic-like fluid source of the Chingshui geothermal field, NE Taiwan evidenced by carbonate clumped-isotope paleothermometry. *Journal of Asian Earth Sciences*. doi:10.1016/j.jseaes.2017.03.004
- Mantilla, L. C., Silva, A., Serrano, J. J., Conde, J., Gomez, C., Ramirez, J. C., . . . Pena, E. (2007) Investigación petrográfica y geoquímica de las sedimentitas del cretácico inferior (k1) y sus manifestaciones hidrotermales asociadas; planchas 169, 170, 189, 190 (cordillera oriental): implicaciones en la búsqueda de esmeraldas. *Ministerio de minas y energía*.

- Mora, A., Parra, M., Strecker, M. R., Sobel, E. R., Hooghiemstra, H., Torres, V., & Jaramillo, J. V. (2008). Climatic forcing of asymmetric orogenic evolution in the Eastern Cordillera of Colombia. *Geological Society of America Bulletin*, 120(7-8), 930-949. doi:10.1130/b26186.1
- Mora, A., Parra, M., Strecker, M. R., Kammer, A., Dimaté, C., & Rodríguez, F. (2006). Cenozoic contractional reactivation of Mesozoic extensional structures in the Eastern Cordillera of Colombia. *Tectonics*, 25(2). doi:10.1029/2005tc001854
- Ottaway, T. L., Wicks, F. J., Bryndzia, L. T., Kyser, T. K., & Spooner, E. T. (1994). Formation of the Muzo hydrothermal emerald deposit in Colombia. *Nature*, 369(6481), 552-554. doi:10.1038/369552a0
- Pignatelli, I., Giuliani, G., Ohnenstetter, D., Agrosi, G., Mathieu, S., Morlot, C., & Branquet, Y. (2015). Colombian Trapiche Emeralds: Recent Advances in Understanding Their Formation. *Gems & Gemology*. doi:10.5741/gems.51.3.222
- Puerto, J. I., Fernandez, J., Pantorrilla, A. (2012) Caracterización mineralógica y estructural de la mina de esmeraldas la pita (Boyacá- Colombia). *Universidad Nacional de Colombia*.
- Reyes, G., Montoya, D., Terraza, R., Fuquen, Jaime., Mayorga, M., (2006) Memoria geología del cinturón esmeraldífero occidental. Ingeominas.
- Rollinson, H. R. (1993). *Using geochemical data: evaluation, presentation, interpretation*. Harlow, Essex u.a.: Longman Scientific & Techn. u.a.

- White, N. C., & Hedenquist, J. W. (1990). Epithermal environments and styles of mineralization: Variations and their causes, and guidelines for exploration. *Journal of Geochemical Exploration*, 36(1-3), 445-474. doi:10.1016/0375-6742(90)90063-g
- 